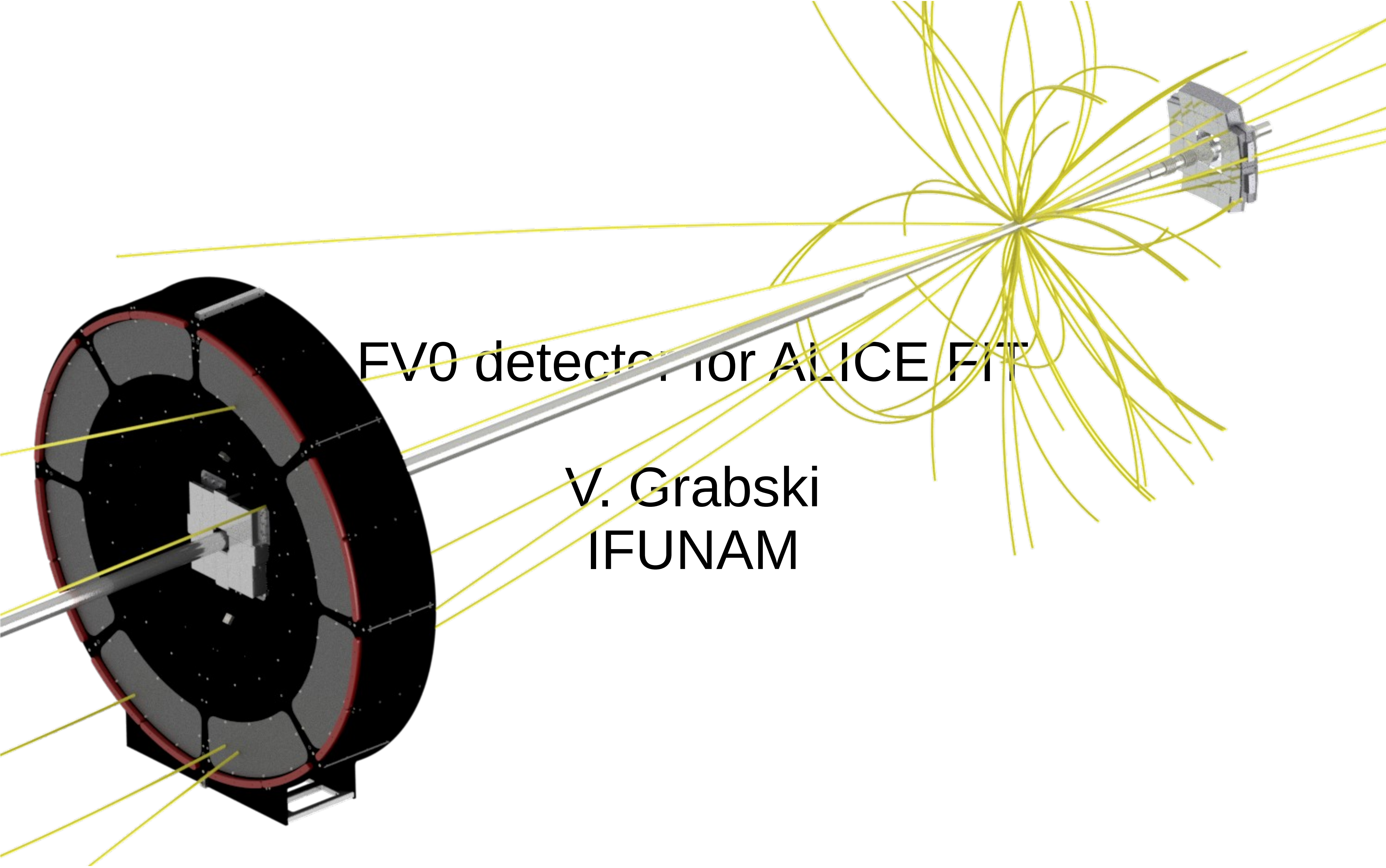

FV0 detector for ALICE FIT

V. Grabski
IFUNAM

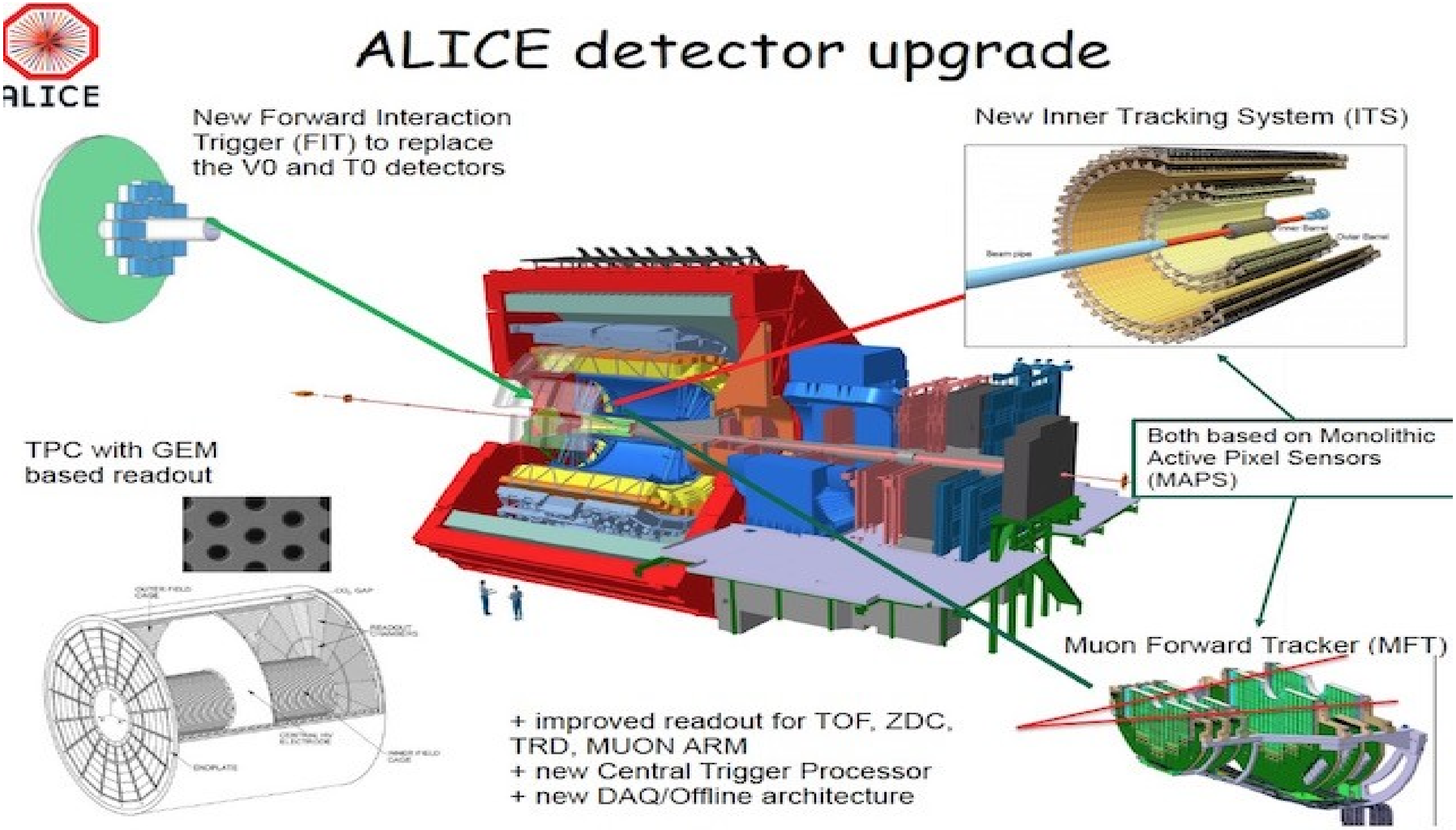

ALICE detector upgrade

New Forward Interaction Trigger (FIT) to replace the V0 and T0 detectors

New Inner Tracking System (ITS)

TPC with GEM based readout

Both based on Monolithic Active Pixel Sensors (MAPS)

Muon Forward Tracker (MFT)

+ improved readout for TOF, ZDC, TRD, MUON ARM
+ new Central Trigger Processor
+ new DAQ/Offline architecture

Collaboration ALICE FIT

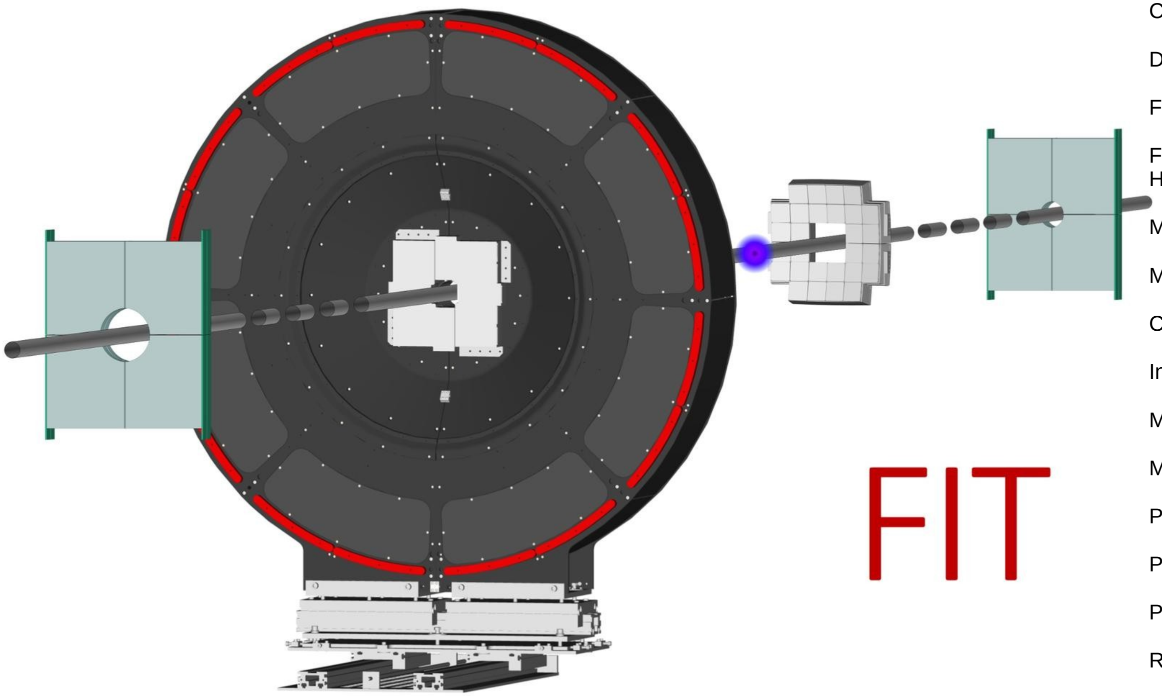

Austria,Vienna,Stefan Meyer Institute

Czech,Praha, Technical University

Denmark,Copenhagen,Niels Bohr Institute, University of Copenhagen

Finland,Helsinki Institute of Physics (HIP) and Univ. of Jyväskylä

Finland Helsinki
Helsinki Institute of Physics (HIP) and Univ. of Helsinki

Mexico Mexico City Instituto de Física, UNAM

Mexico Mexico City and Merida

CINVESTAV, Mexico Mexico City

Instituto de Ciencias Nucleares, UNAM

Mexico,Puebla,Benemérita Universidad Autónoma de Puebla

Mexico,Culiacan, Sinaloa,Universidad Autónoma de Sinaloa

Peru Lima,Pontificia Universidad Católica del Perú

Poland Krakow ,AGH,Poland,Krakow IFJ-PAN

Poland Warsaw ,NCBJ

Russia Moscow,Institute for Nuclear Research

Russia Moscow,Moscow Engineering Physics Institute

Russia Moscow,Russian Research Centre Kurchatov Institute

USA Chicago ,Chicago State University

USA San Luis Obispo,California Polytechnic State University

https://alice-collaboration.web.cern.ch/menu_proj_items/FIT

The main purpose of the FIT

- Time reference for the other detectors;
- Vertex and collision rate estimation;
- Luminosity Monitor
- Residual gas background estimation;
- Collision centrality estimation;
- Estimation of the reaction plane;
- Different triggers for the data analysis;

Detectors acceptances in Pseudorapidity

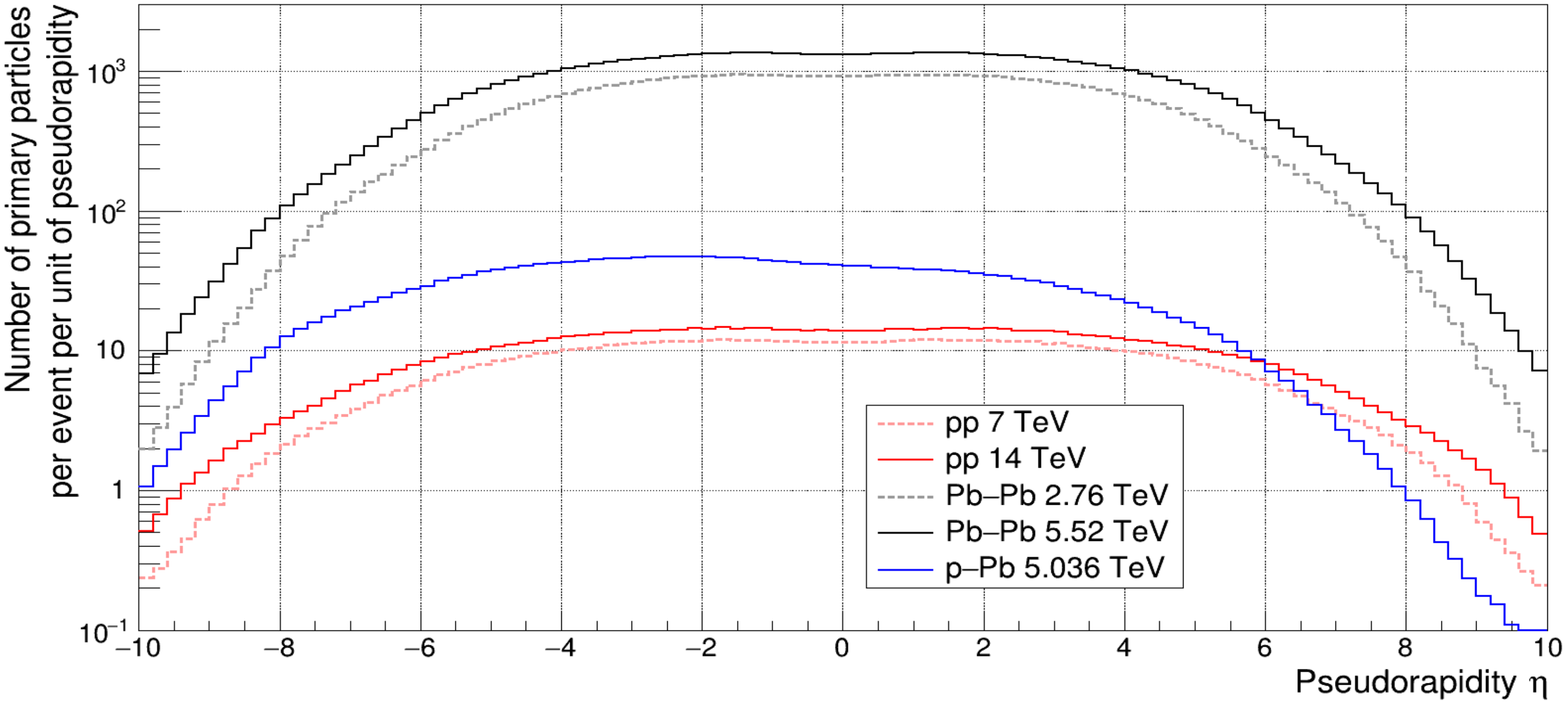

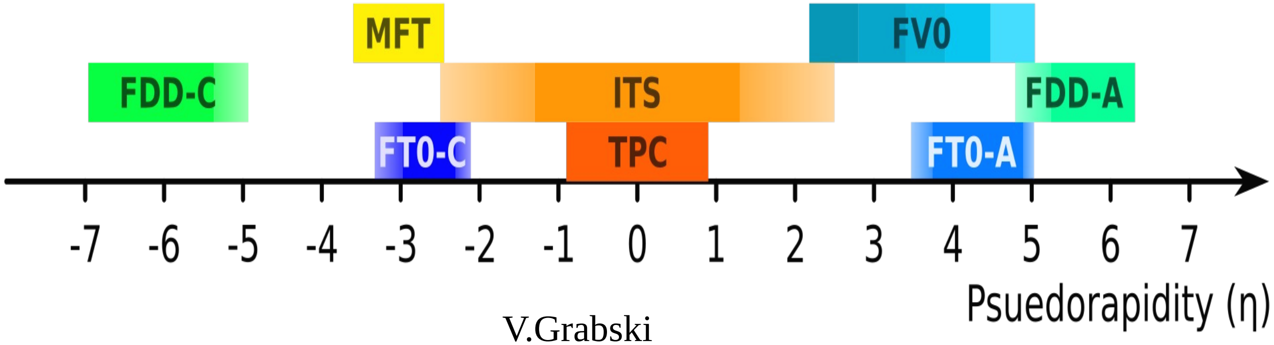

V0A and V0C detectors

Time resolution 200ps

Mexico

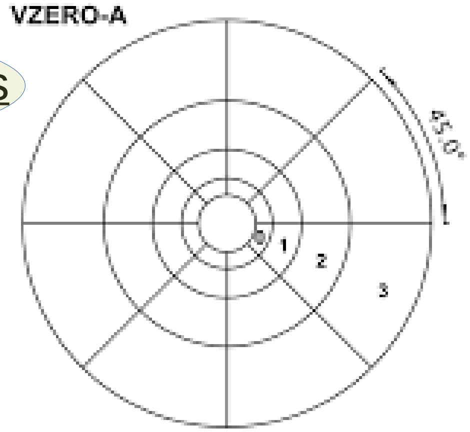

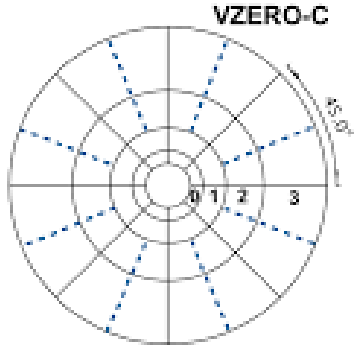

Francia

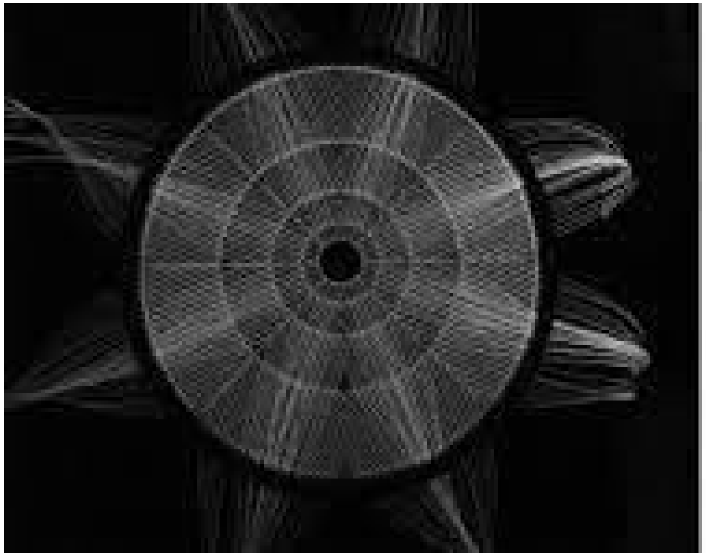

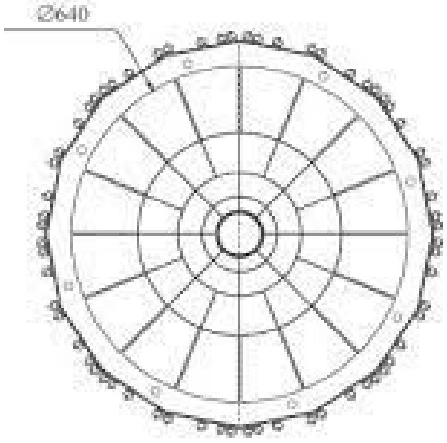

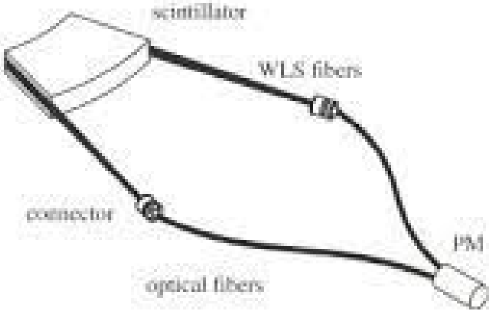

A new design for the FV0 detector

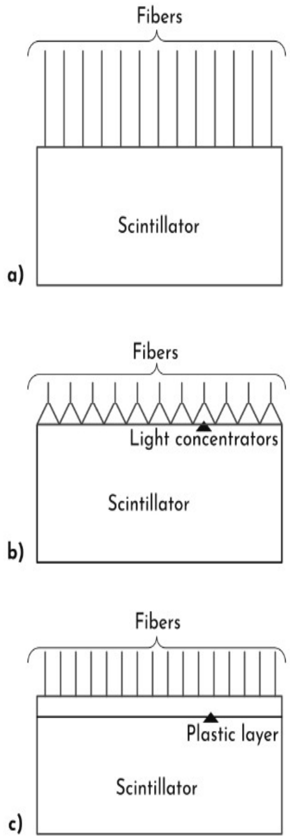

Figure D.1: Three different light collection schemes.

New fiber read-out design for the large area scintillator detectors: providing good amplitude and time resolutions

V. Grabski[1]

Instituto de Fisica Universidad Nacional Autonoma de Mexico, Mexico

[a]*Av Universidad 3000, Instituto de Fisica, Coyoacan, Mexico*

Abstract

Most of the time-of-flight systems as well as the fast interaction trigger detectors have large surfaces and the principal requirements for the above mentioned detectors is a good time resolution of the order $100-200ps$. The easiest solution here is to split the large surface into the small tiles with a read-out directly attached to the photo-sensor. This solution is expensive because the number of the channels grows proportional to the surface. Although if the coverage of the whole surface by the sensors is not sufficient, one can obtain non uniform response, which is not acceptable if uniformity is required. Our suggestion is based on the usage of clear fibres mounted perpendicular on the surface of the scintillator as a matrix providing uniform surface reduction and keeping most of the benefices of the small tiles with the photo-sensors. In this work the design and some analytic estimations of the light collection efficiency for direct and reflected photons will be presented. Also some simple estimations are presented for the time-spread and for the light pulse wave form dependent on the lateral sizes and the thickness of the scintillator.

Keywords: `Scintillation detector, Time-of-flight detector, Particle identification, Fast Interaction Trigger, Optical Fibre`

---

[*] Corresponding author
Email address: `varlen.grabski@cern.ch` (V. Grabski)

Preprint submitted to Journal of LATEX Templates *September 4, 2019*

A new design for the FV0 detector

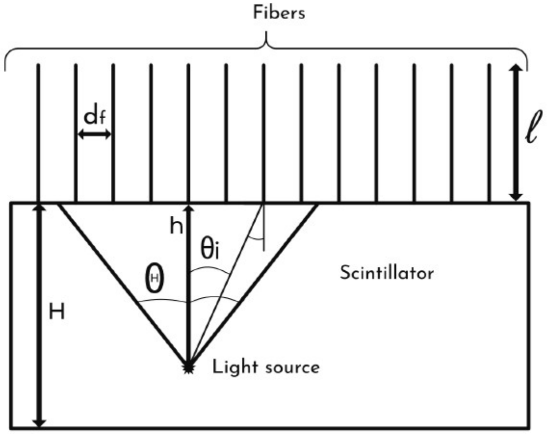

Figure D.2: Light collection scheme from the point like source for direct photons. Description of all notations are in the text.

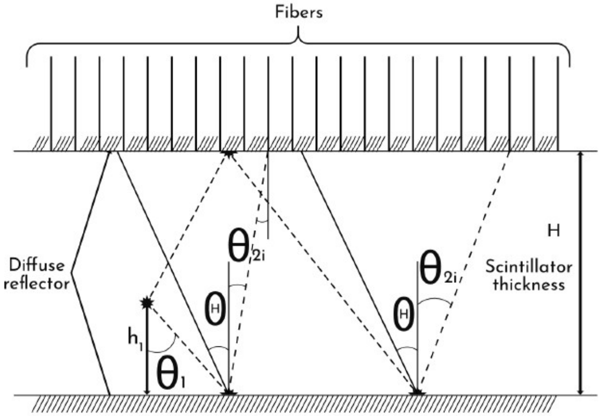

Figure D.3: Light collection scheme from the point like source and for the reflected photons. Description of all notations are in the text.

22

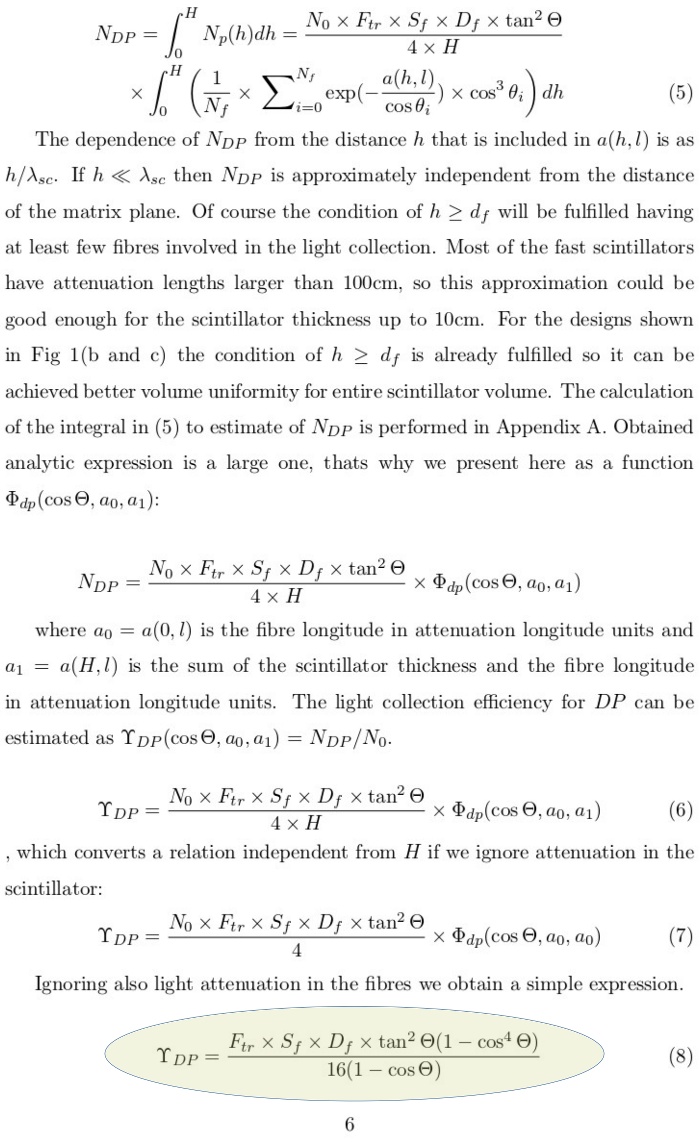

$$N_{DP} = \int_0^H N_p(h)dh = \frac{N_0 \times F_{tr} \times S_f \times D_f \times \tan^2\Theta}{4 \times H}$$
$$\times \int_0^H \left(\frac{1}{N_f} \times \sum\nolimits_{i=0}^{N_f} \exp(-\frac{a(h,l)}{\cos\theta_i}) \times \cos^3\theta_i\right) dh \qquad (5)$$

The dependence of N_{DP} from the distance h that is included in $a(h,l)$ is as h/λ_{sc}. If $h \ll \lambda_{sc}$ then N_{DP} is approximately independent from the distance of the matrix plane. Of course the condition of $h \geq d_f$ will be fulfilled having at least few fibres involved in the light collection. Most of the fast scintillators have attenuation lengths larger than 100cm, so this approximation could be good enough for the scintillator thickness up to 10cm. For the designs shown in Fig 1(b and c) the condition of $h \geq d_f$ is already fulfilled so it can be achieved better volume uniformity for entire scintillator volume. The calculation of the integral in (5) to estimate of N_{DP} is performed in Appendix A. Obtained analytic expression is a large one, thats why we present here as a function $\Phi_{dp}(\cos\Theta, a_0, a_1)$:

$$N_{DP} = \frac{N_0 \times F_{tr} \times S_f \times D_f \times \tan^2\Theta}{4 \times H} \times \Phi_{dp}(\cos\Theta, a_0, a_1)$$

where $a_0 = a(0,l)$ is the fibre longitude in attenuation longitude units and $a_1 = a(H,l)$ is the sum of the scintillator thickness and the fibre longitude in attenuation longitude units. The light collection efficiency for DP can be estimated as $\Upsilon_{DP}(\cos\Theta, a_0, a_1) = N_{DP}/N_0$.

$$\Upsilon_{DP} = \frac{N_0 \times F_{tr} \times S_f \times D_f \times \tan^2\Theta}{4 \times H} \times \Phi_{dp}(\cos\Theta, a_0, a_1) \qquad (6)$$

, which converts a relation independent from H if we ignore attenuation in the scintillator:

$$\Upsilon_{DP} = \frac{N_0 \times F_{tr} \times S_f \times D_f \times \tan^2\Theta}{4} \times \Phi_{dp}(\cos\Theta, a_0, a_0) \qquad (7)$$

Ignoring also light attenuation in the fibres we obtain a simple expression.

$$\Upsilon_{DP} = \frac{F_{tr} \times S_f \times D_f \times \tan^2\Theta(1-\cos^4\Theta)}{16(1-\cos\Theta)} \qquad (8)$$

6

A new design for the FV0 detector

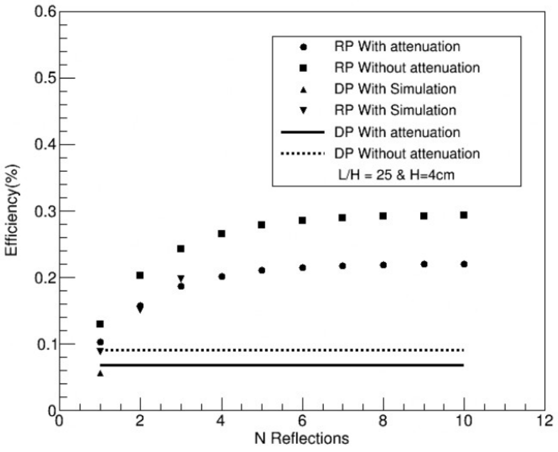

Figure D.4: Light collection efficiency vs number of reflections. Lines show efficiency for DP with and without attenuation in the scintillator and in the fibres

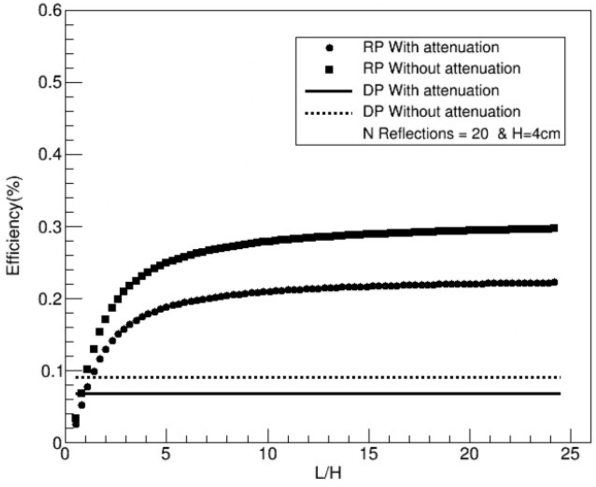

Figure D.5: Light collection efficiency vs detector lateral sizes in the scintillator thickness units.

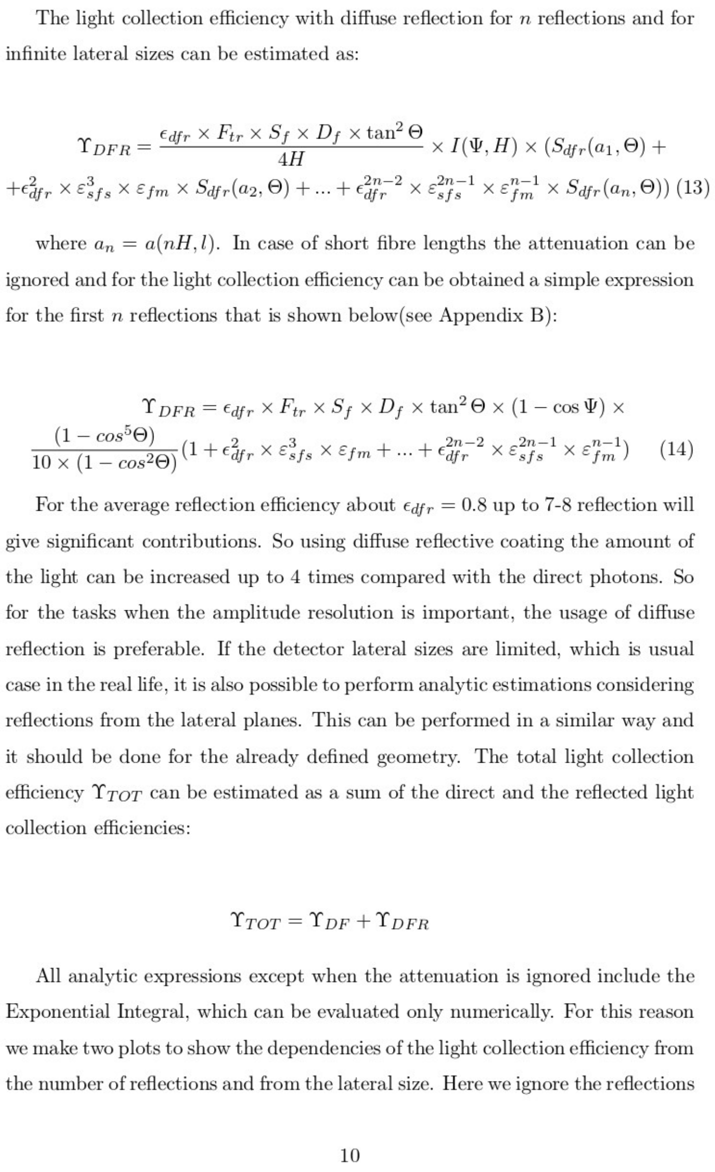

The light collection efficiency with diffuse reflection for n reflections and for infinite lateral sizes can be estimated as:

$$\Upsilon_{DFR} = \frac{\epsilon_{dfr}\times F_{tr}\times S_f\times D_f\times\tan^2\Theta}{4H}\times I(\Psi,H)\times(S_{dfr}(a_1,\Theta)+ +\epsilon^2_{dfr}\times\varepsilon^3_{sfs}\times\varepsilon_{fm}\times S_{dfr}(a_2,\Theta)+...+\epsilon^{2n-2}_{dfr}\times\varepsilon^{2n-1}_{sfs}\times\varepsilon^{n-1}_{fm}\times S_{dfr}(a_n,\Theta)) \quad (13)$$

where $a_n = a(nH, l)$. In case of short fibre lengths the attenuation can be ignored and for the light collection efficiency can be obtained a simple expression for the first n reflections that is shown below(see Appendix B):

$$\Upsilon_{DFR}=\epsilon_{dfr}\times F_{tr}\times S_f\times D_f\times\tan^2\Theta\times(1-\cos\Psi)\times \frac{(1-cos^5\Theta)}{10\times(1-cos^2\Theta)}(1+\epsilon^2_{dfr}\times\varepsilon^3_{sfs}\times\varepsilon_{fm}+...+\epsilon^{2n-2}_{dfr}\times\varepsilon^{2n-1}_{sfs}\times\varepsilon^{n-1}_{fm}) \quad (14)$$

For the average reflection efficiency about $\epsilon_{dfr} = 0.8$ up to 7-8 reflection will give significant contributions. So using diffuse reflective coating the amount of the light can be increased up to 4 times compared with the direct photons. So for the tasks when the amplitude resolution is important, the usage of diffuse reflection is preferable. If the detector lateral sizes are limited, which is usual case in the real life, it is also possible to perform analytic estimations considering reflections from the lateral planes. This can be performed in a similar way and it should be done for the already defined geometry. The total light collection efficiency Υ_{TOT} can be estimated as a sum of the direct and the reflected light collection efficiencies:

$$\Upsilon_{TOT} = \Upsilon_{DF} + \Upsilon_{DFR}$$

All analytic expressions except when the attenuation is ignored include the Exponential Integral, which can be evaluated only numerically. For this reason we make two plots to show the dependencies of the light collection efficiency from the number of reflections and from the lateral size. Here we ignore the reflections

10

A new design for the FV0 detector

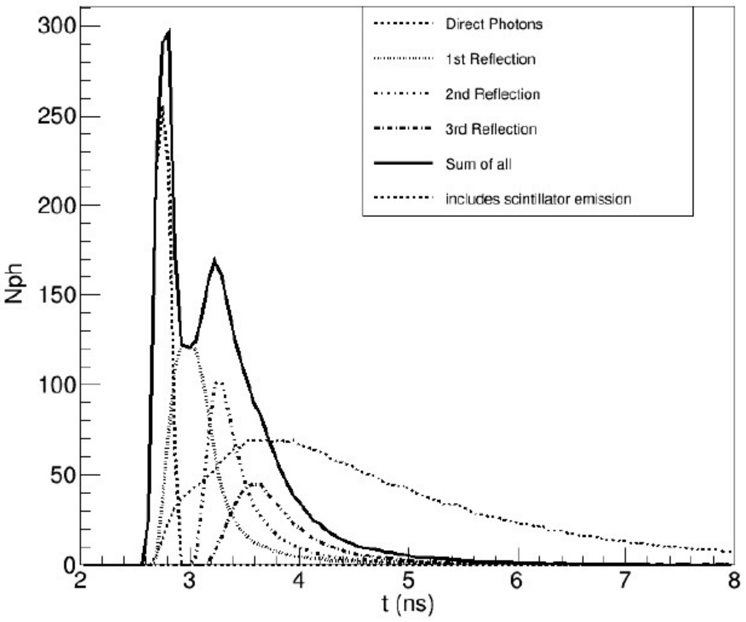

Figure D.6: Pulse time wave forms for direct and reflected photons.

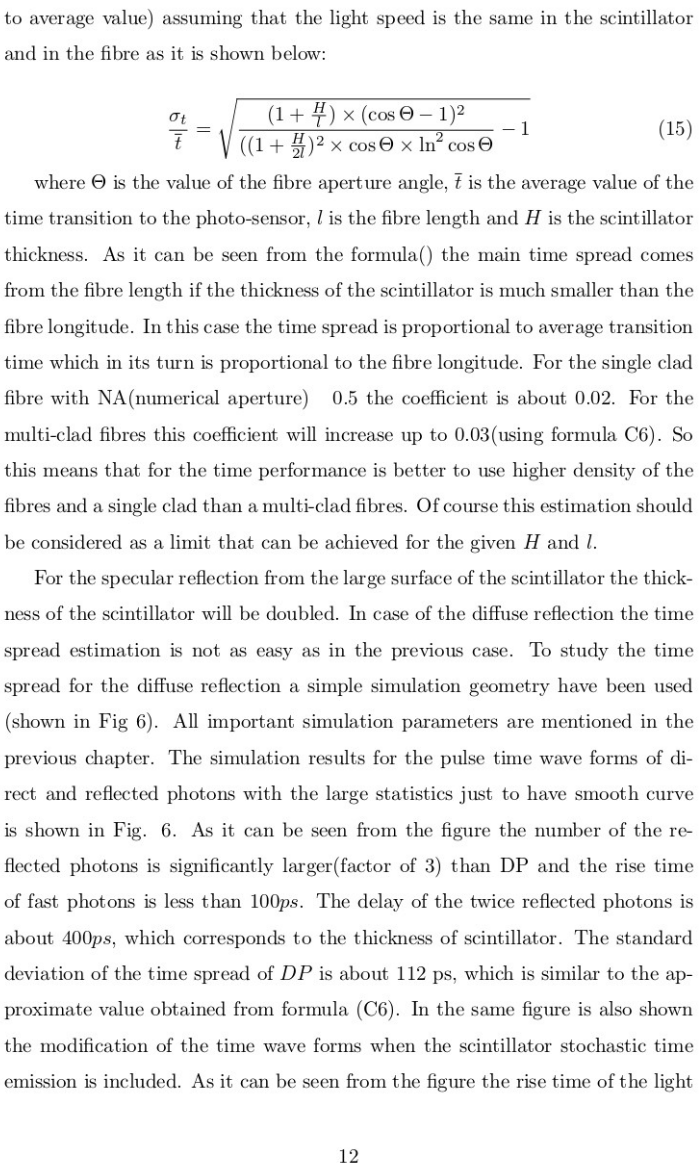

to average value) assuming that the light speed is the same in the scintillator and in the fibre as it is shown below:

$$\frac{\sigma_t}{\bar{t}} = \sqrt{\frac{(1+\frac{H}{l})\times(\cos\Theta-1)^2}{((1+\frac{H}{2l})^2\times\cos\Theta\times\ln^2\cos\Theta} - 1} \tag{15}$$

where Θ is the value of the fibre aperture angle, $\bar{t}$ is the average value of the time transition to the photo-sensor, l is the fibre length and H is the scintillator thickness. As it can be seen from the formula() the main time spread comes from the fibre length if the thickness of the scintillator is much smaller than the fibre longitude. In this case the time spread is proportional to average transition time which in its turn is proportional to the fibre longitude. For the single clad fibre with NA(numerical aperture) 0.5 the coefficient is about 0.02. For the multi-clad fibres this coefficient will increase up to 0.03(using formula C6). So this means that for the time performance is better to use higher density of the fibres and a single clad than a multi-clad fibres. Of course this estimation should be considered as a limit that can be achieved for the given H and l.

For the specular reflection from the large surface of the scintillator the thickness of the scintillator will be doubled. In case of the diffuse reflection the time spread estimation is not as easy as in the previous case. To study the time spread for the diffuse reflection a simple simulation geometry have been used (shown in Fig 6). All important simulation parameters are mentioned in the previous chapter. The simulation results for the pulse time wave forms of direct and reflected photons with the large statistics just to have smooth curve is shown in Fig. 6. As it can be seen from the figure the number of the reflected photons is significantly larger(factor of 3) than DP and the rise time of fast photons is less than $100ps$. The delay of the twice reflected photons is about $400ps$, which corresponds to the thickness of scintillator. The standard deviation of the time spread of DP is about 112 ps, which is similar to the approximate value obtained from formula (C6). In the same figure is also shown the modification of the time wave forms when the scintillator stochastic time emission is included. As it can be seen from the figure the rise time of the light

Detector Construction

Choice of construction materials

- Scintillator
- Optical Fiber
- Photo-sensor

Scintillator

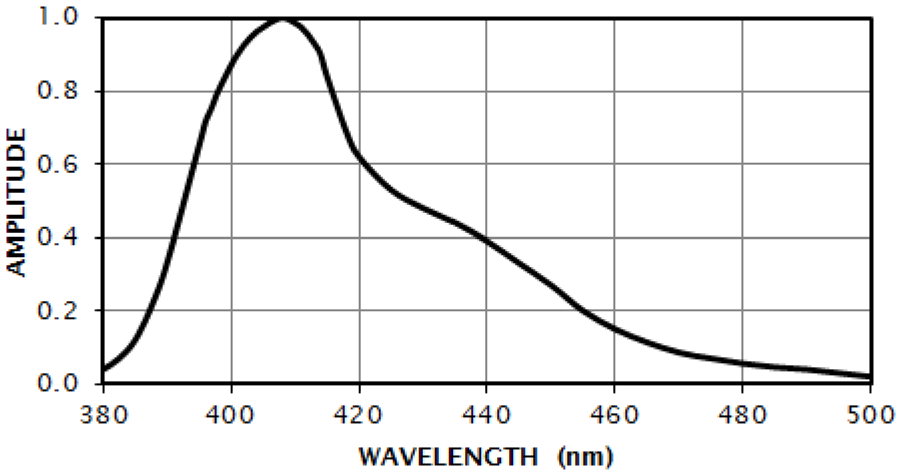

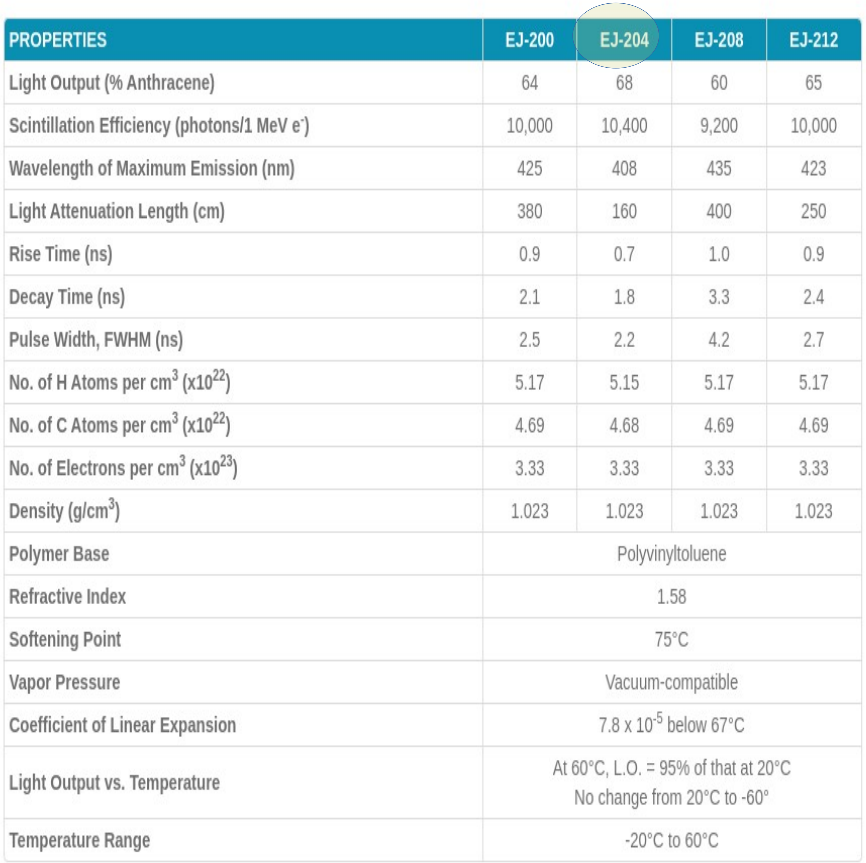

PROPERTIES	EJ-200	EJ-204	EJ-208	EJ-212
Light Output (% Anthracene)	64	68	60	65
Scintillation Efficiency (photons/1 MeV e$^-$)	10,000	10,400	9,200	10,000
Wavelength of Maximum Emission (nm)	425	408	435	423
Light Attenuation Length (cm)	380	160	400	250
Rise Time (ns)	0.9	0.7	1.0	0.9
Decay Time (ns)	2.1	1.8	3.3	2.4
Pulse Width, FWHM (ns)	2.5	2.2	4.2	2.7
No. of H Atoms per cm^3 (x10^{22})	5.17	5.15	5.17	5.17
No. of C Atoms per cm^3 (x10^{22})	4.69	4.68	4.69	4.69
No. of Electrons per cm^3 (x10^{23})	3.33	3.33	3.33	3.33
Density (g/cm^3)	1.023	1.023	1.023	1.023
Polymer Base	Polyvinyltoluene			
Refractive Index	1.58			
Softening Point	75°C			
Vapor Pressure	Vacuum-compatible			
Coefficient of Linear Expansion	7.8 x 10^{-5} below 67°C			
Light Output vs. Temperature	At 60°C, L.O. = 95% of that at 20°C No change from 20°C to -60°			
Temperature Range	-20°C to 60°C			

PROPERTIES	EJ-228	EJ-230
Light Output (% Anthracene)	67	64
Scintillation Efficiency (photons/1 MeV e-)	10,200	9,700
Wavelength of Maximum Emission (nm)	391	391
Light Attenuation Length (cm)	-	120
Rise Time (ns)	0.5	0.5
Decay Time (ns)	1.4	1.5
Pulse Width, FWHM (ns)	1.2	1.3
No. of H Atoms per cm3 (x1022)	5.15	5.15
No. of C Atoms per cm3 (x1022)	4.69	4.69
No. of Electrons per cm3 (x1023)	3.33	3.33
Density (g/cm3)	1.023	1.023

Prototype 2 with cosmic muons New cheap EJ204 tests

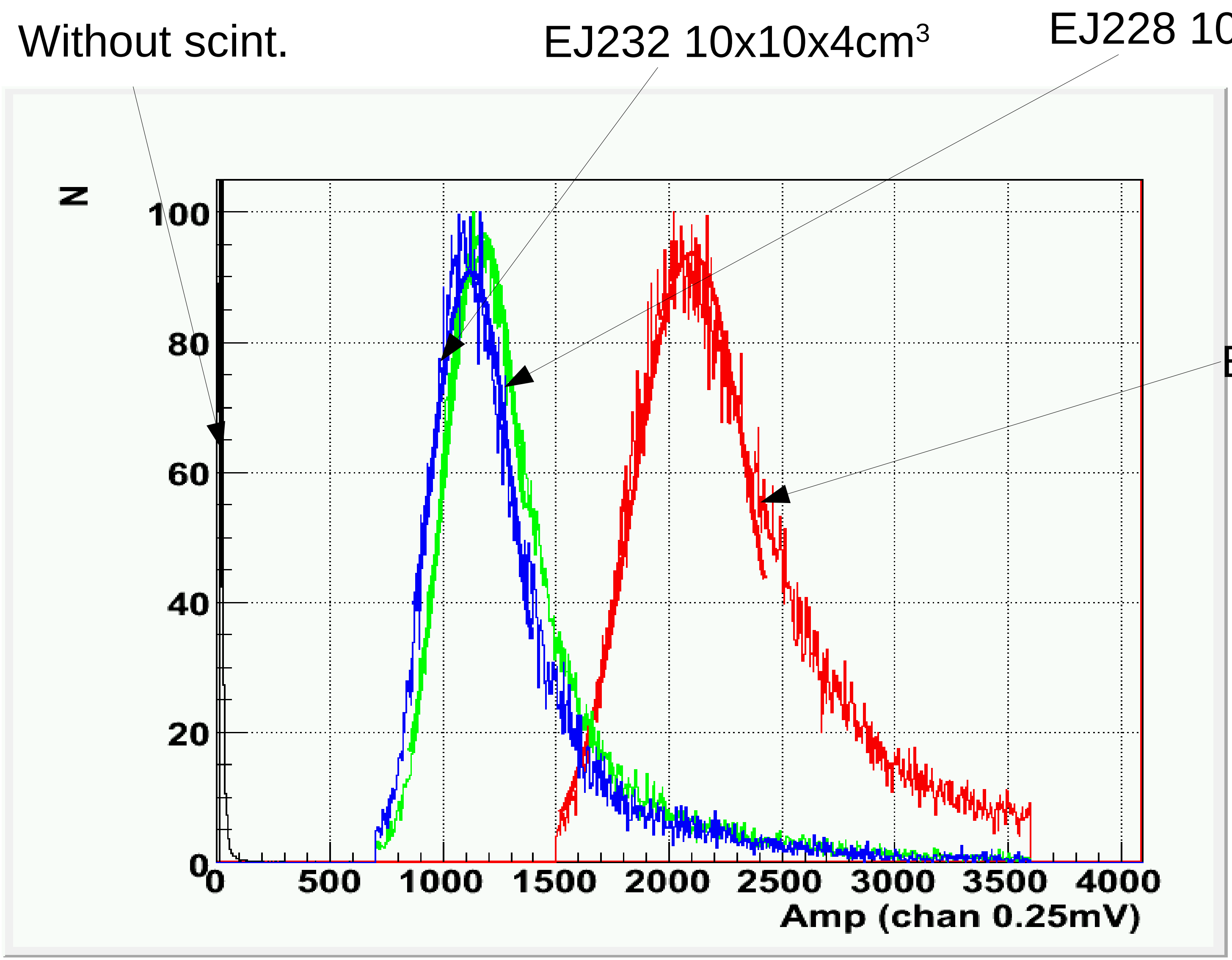
Without scint.

EJ232 10x10x4cm^3

EJ228 10x10x4cm^3

EJ204 10x10x4cm^3

Small amplitude from EJ232&EJ228 due to absorption

All scintillators are painted
Opt. Grass. Is applied
in both side of fibers

Optical Fibers

Kuraray and Bycron for the science

Kuraray and Bycron better quality, but more expensive

Commercials
Asahi, Mitsubishi
Etc.

The commercial ones from 5 to 10 times cheaper

Asahi

Configuration: Simplex

Core Diameter: 1.0mm

Core Material: PMMA (Polymethyl Methacrylate)

Numerical Aperture: 0.6

Attenuation: 0.19 dB/m at 650 nm

Operating Temperature Range: -55Â°C to 85Â°C

Mitsubishi

Configuration: Simplex

Core Diameter: 1.0mm

Core Material: PMMA (Polymethyl Methacrylate)

Numerical Aperture: 0.5

Attenuation: 0.20 dB/m at 650 nm

Operating Temperature Range: -55Â°C to 70Â°C

Kuraray

Configuration: Simplex

Core Diameter: 1.0mm

Core Material: ?

Numerical Aperture: 0.55

Attenuation: ?

Operating Temperature Range: ?

Photo-sensors

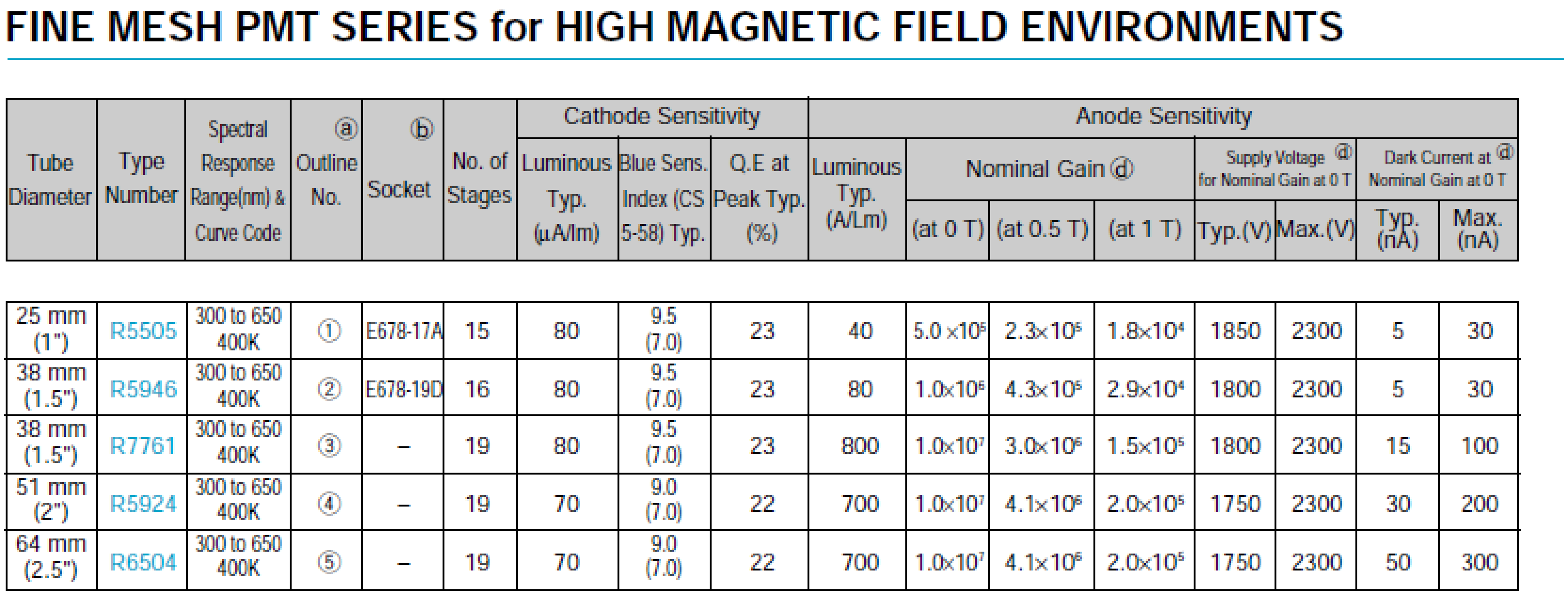

FINE MESH PMT SERIES for HIGH MAGNETIC FIELD ENVIRONMENTS

Tube Diameter	Type Number	Spectral Response Range(nm) & Curve Code	ⓐ Outline No.	ⓑ Socket	No. of Stages	Cathode Sensitivity			Anode Sensitivity							
						Luminous Typ. (µA/lm)	Blue Sens. Index (CS 5-58) Typ.	Q.E at Peak Typ. (%)	Luminous Typ. (A/Lm)	Nominal Gain ⓓ			Supply Voltage ⓓ for Nominal Gain at 0 T		Dark Current at ⓓ Nominal Gain at 0 T	
										(at 0 T)	(at 0.5 T)	(at 1 T)	Typ.(V)	Max.(V)	Typ. (nA)	Max. (nA)
25 mm (1")	R5505	300 to 650 400K	①	E678-17A	15	80	9.5 (7.0)	23	40	5.0×10^5	2.3×10^5	1.8×10^4	1850	2300	5	30
38 mm (1.5")	R5946	300 to 650 400K	②	E678-19D	16	80	9.5 (7.0)	23	80	1.0×10^6	4.3×10^5	2.9×10^4	1800	2300	5	30
38 mm (1.5")	R7761	300 to 650 400K	③	–	19	80	9.5 (7.0)	23	800	1.0×10^7	3.0×10^6	1.5×10^5	1800	2300	15	100
51 mm (2")	R5924	300 to 650 400K	④	–	19	70	9.0 (7.0)	22	700	1.0×10^7	4.1×10^6	2.0×10^5	1750	2300	30	200
64 mm (2.5")	R6504	300 to 650 400K	⑤	–	19	70	9.0 (7.0)	22	700	1.0×10^7	4.1×10^6	2.0×10^5	1750	2300	50	300

SiPM

Radiation
Cheap
FEE

MCP
More expensive
Limited accumulated charge
Limited anode current
Fast and short pulses

Fine mesh options from Hamamatsu

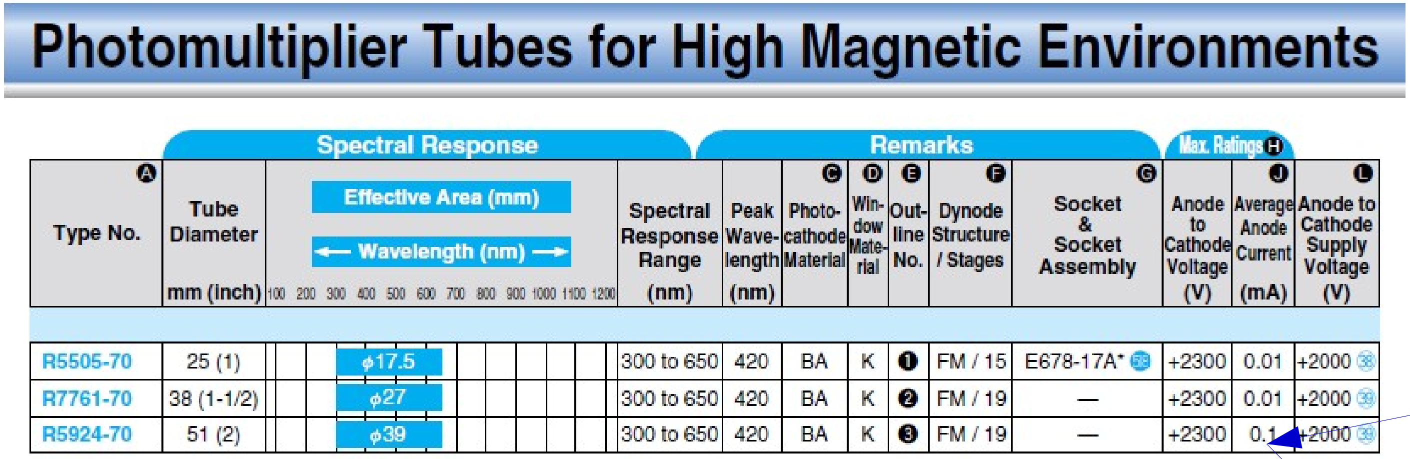

Photomultiplier Tubes for High Magnetic Environments

Ⓐ Type No.	Spectral Response				Remarks					Max. Ratings Ⓗ		
	Tube Diameter mm (inch)	Effective Area (mm) ← Wavelength (nm) → 100 200 300 400 500 600 700 800 900 1000 1100 1200	Spectral Response Range (nm)	Peak Wavelength (nm)	Ⓒ Photocathode Material	Ⓓ Window Material	Ⓔ Outline No.	Ⓕ Dynode Structure / Stages	Ⓖ Socket & Socket Assembly	Anode to Cathode Voltage (V)	Ⓙ Average Anode Current (mA)	Ⓛ Anode to Cathode Supply Voltage (V)
R5505-70	25 (1)	ϕ17.5	300 to 650	420	BA	K	❶	FM / 15	E678-17A* (53)	+2300	0.01	+2000 ㊳
R7761-70	38 (1-1/2)	ϕ27	300 to 650	420	BA	K	❷	FM / 19	—	+2300	0.01	+2000 ㊴
R5924-70	51 (2)	ϕ39	300 to 650	420	BA	K	❸	FM / 19	—	+2300	0.1	+2000 ㊴

Small sizes with maximum average anode current 10uA
And the large one with 100uA

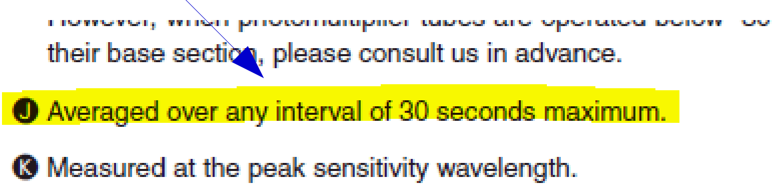

However, when photomultiplier tubes are operated below -30
their base section, please consult us in advance.

Ⓙ Averaged over any interval of 30 seconds maximum.

Ⓚ Measured at the peak sensitivity wavelength.

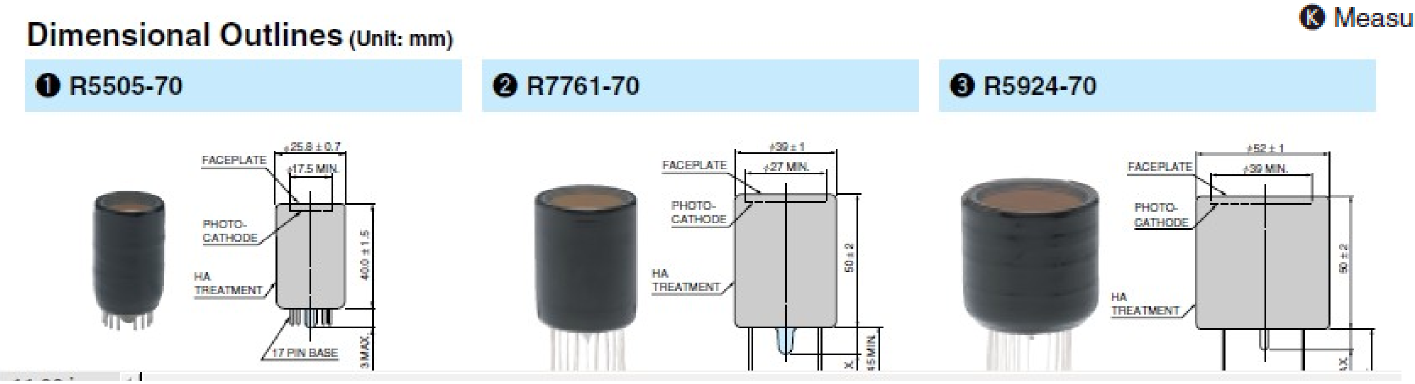

Dimensional Outlines (Unit: mm)

❶ R5505-70

❷ R7761-70

❸ R5924-70

First Prototype

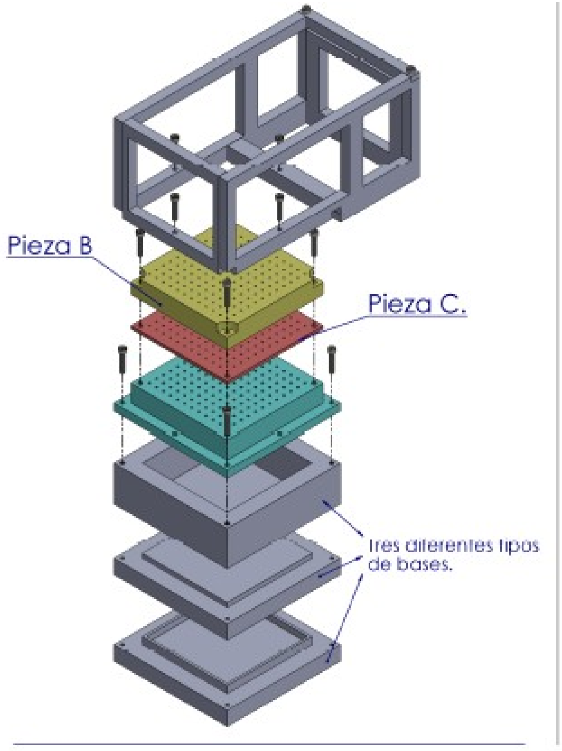

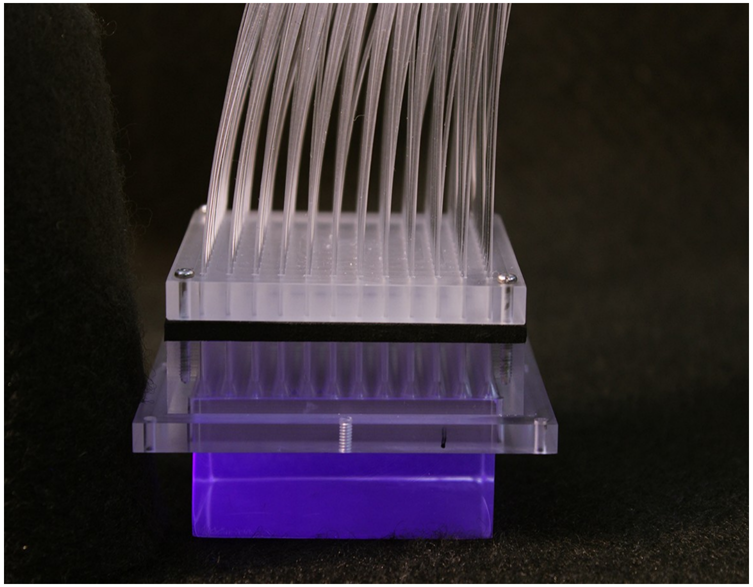

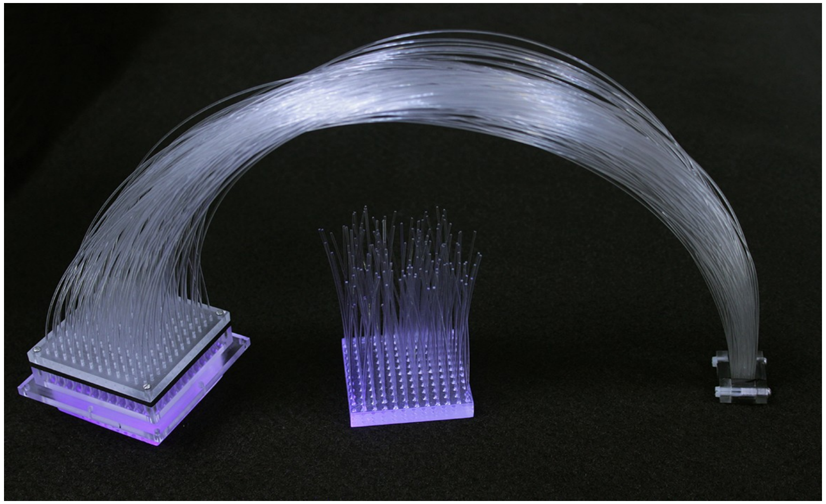

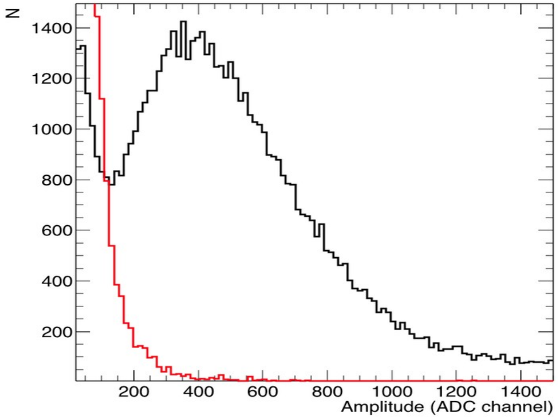

Second Prototype

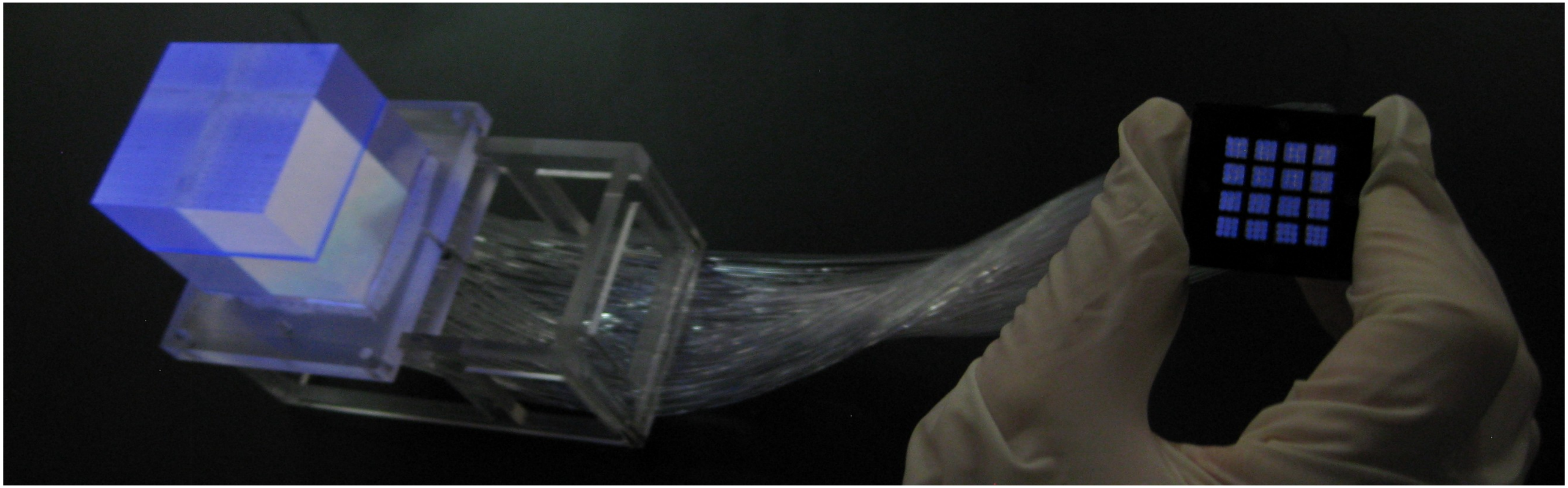

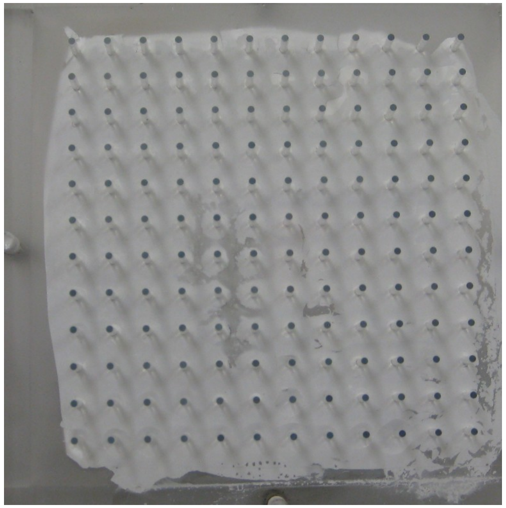

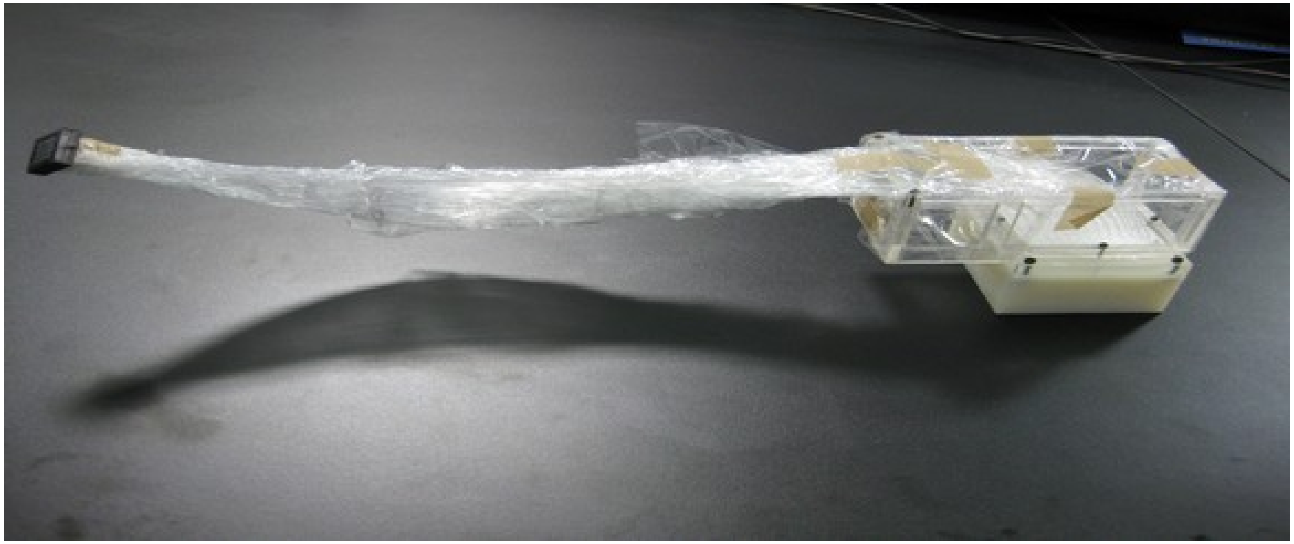

Scintillator coating study

To reach 200ps limit should be increase the light

- The thickness of scintillator
- The density of the fibers

Variation between 30 ps

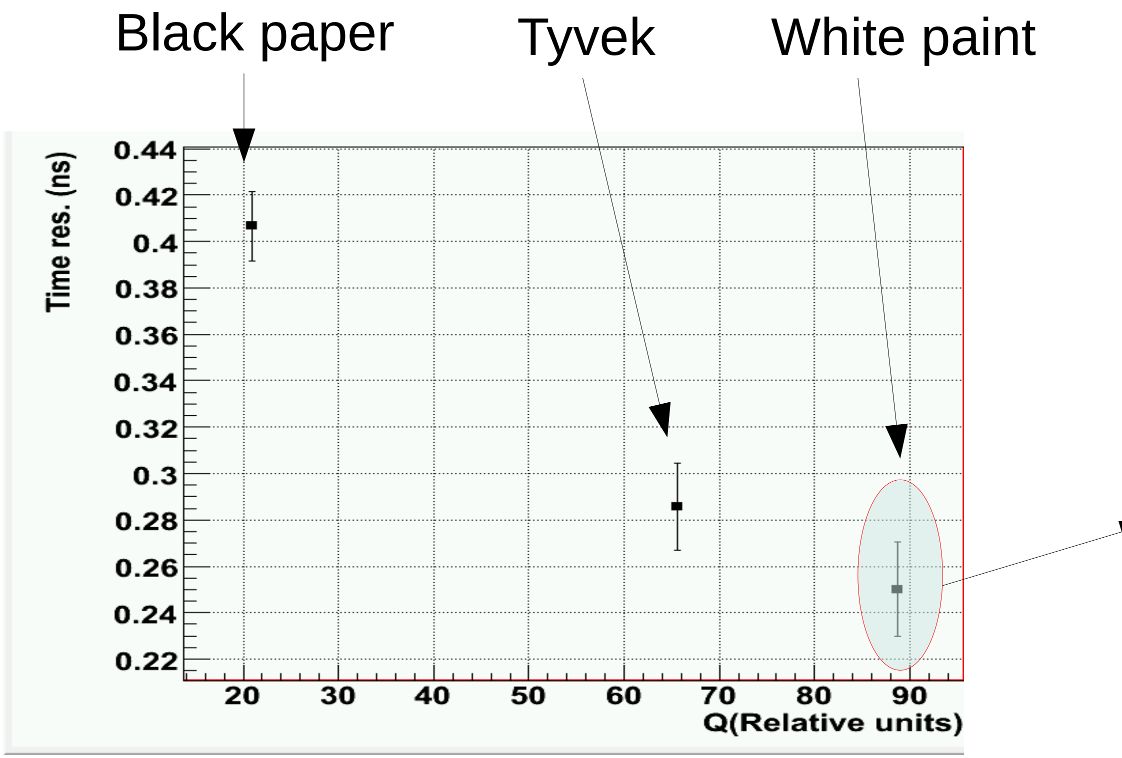

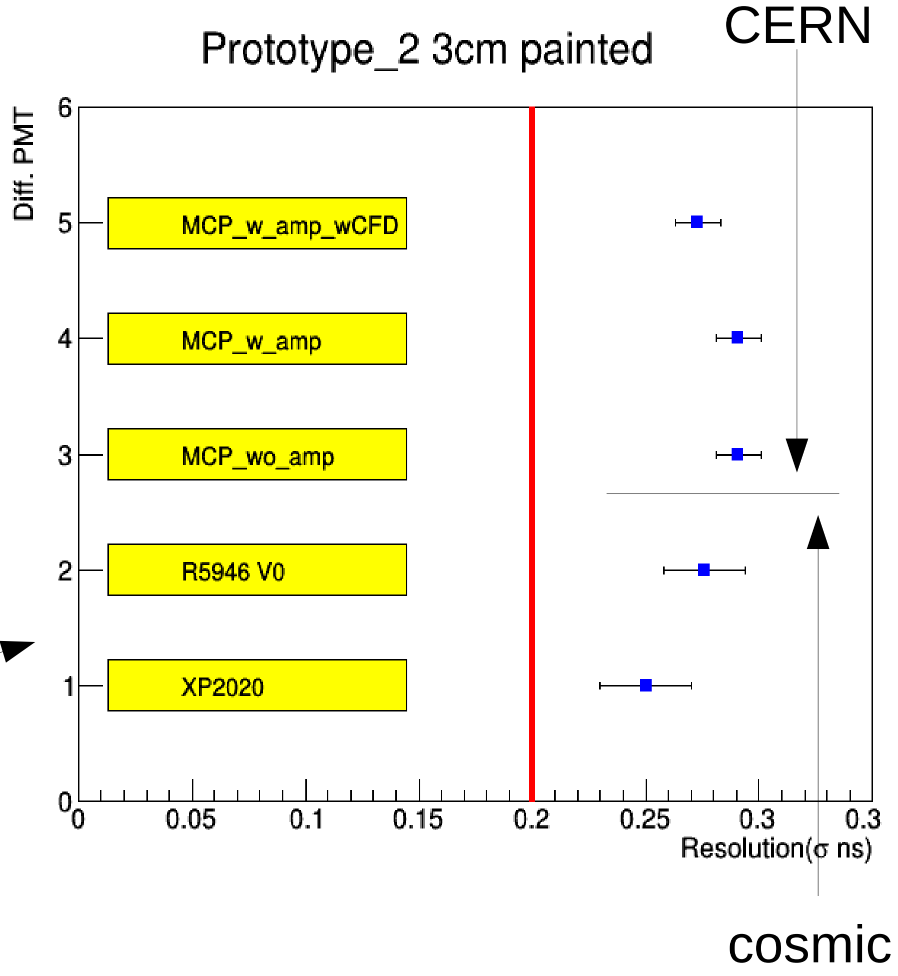

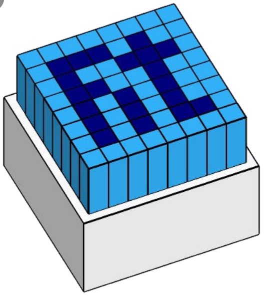

Scintillator thickness study

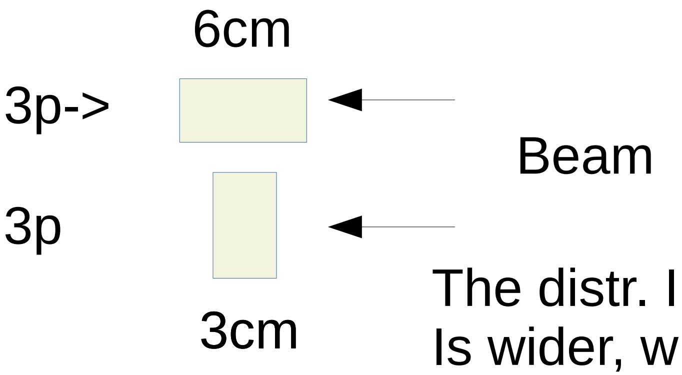

Significant improvement ~40 ps
Using CFD ?
Should be checked our time estimation

The distr. In case of 3p
Is wider, which is expected

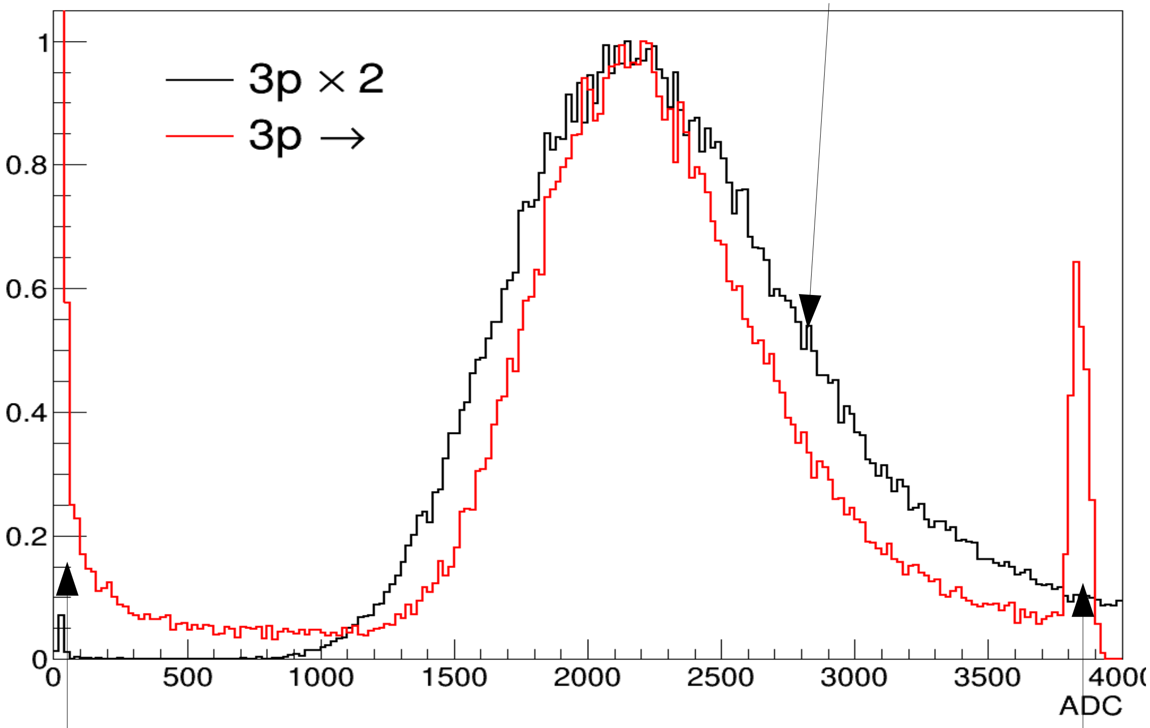

Part of beam is out

ADC saturation

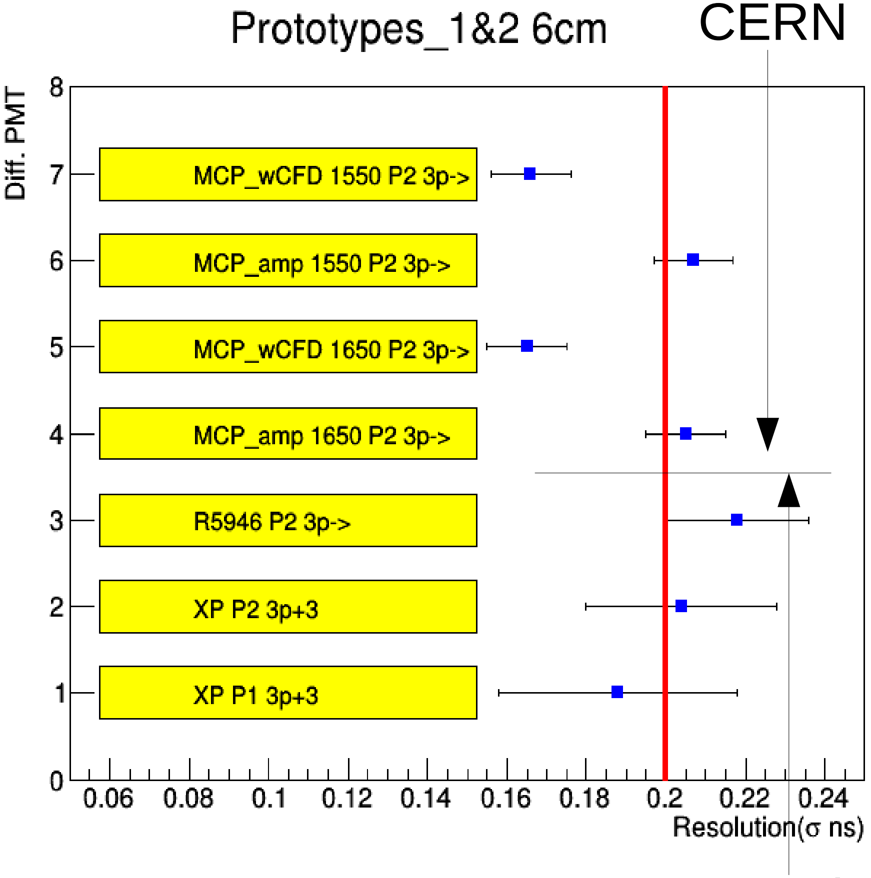

CERN

Cosmic
muons

Third Prototype

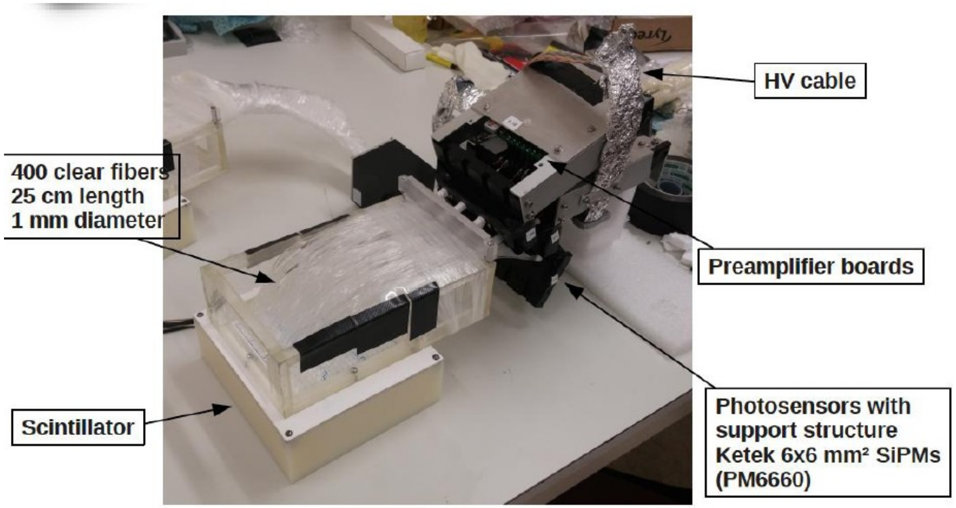

400 clear fibers
25 cm length
1 mm diameter

HV cable

Preamplifier boards

Scintillator

Photosensors with
support structure
Ketek 6x6 mm² SiPMs
(PM6660)

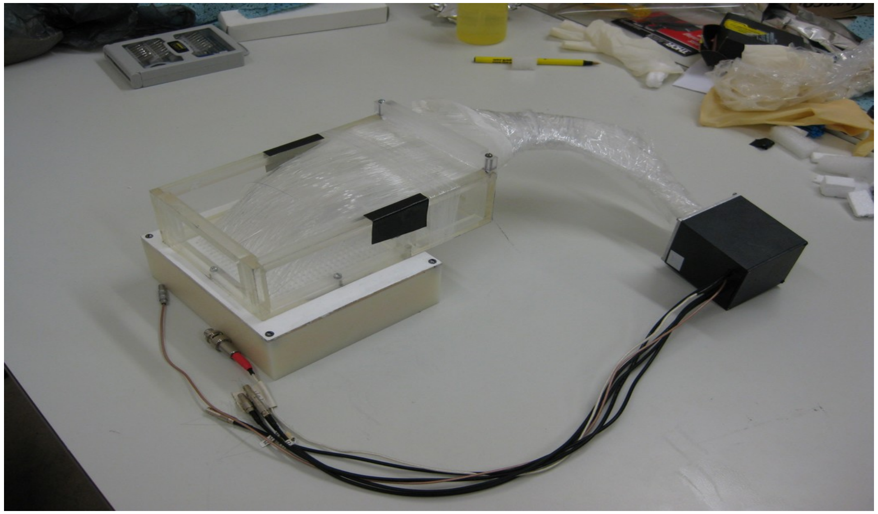

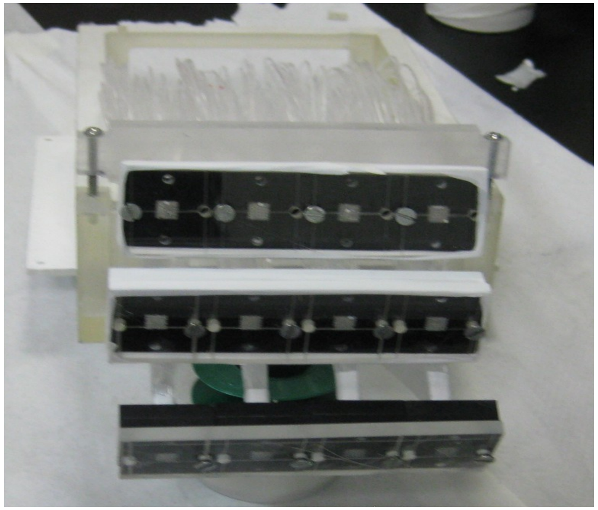

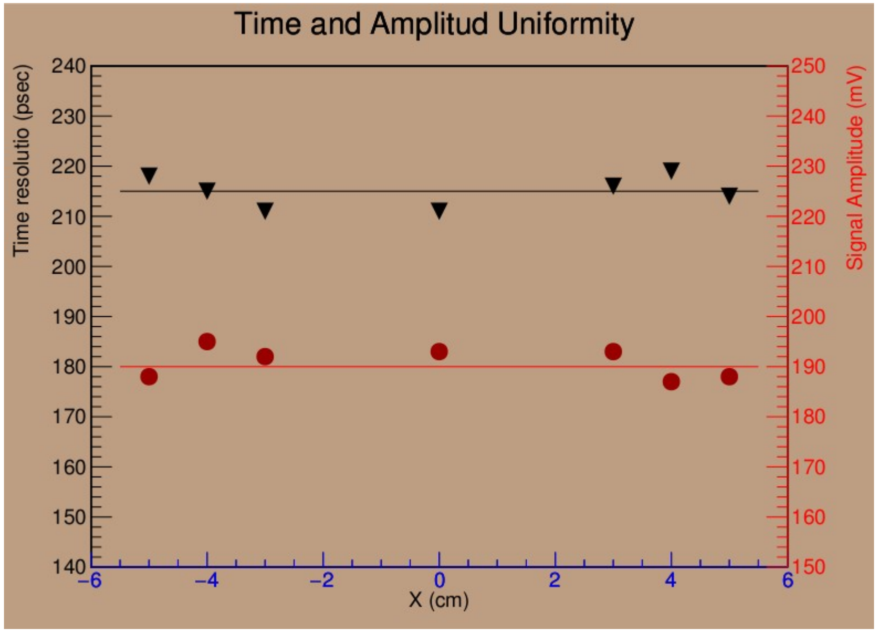

Forth Prototype

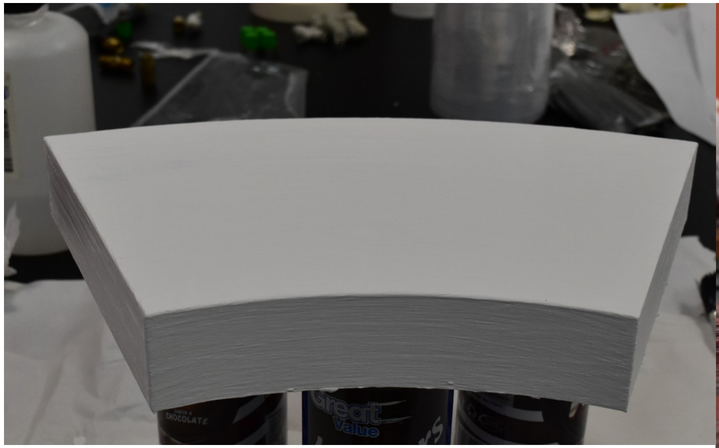

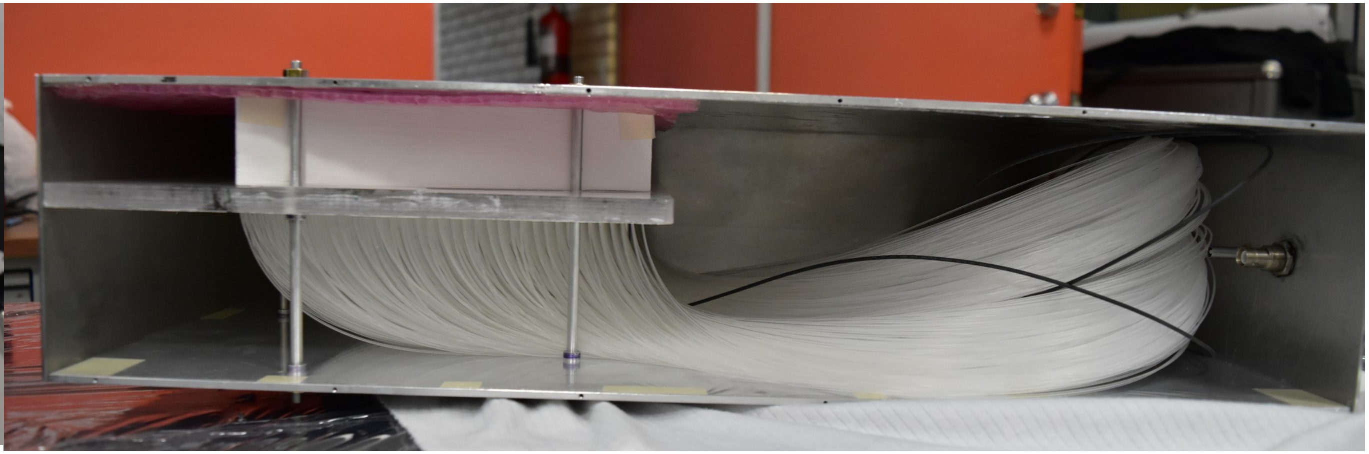

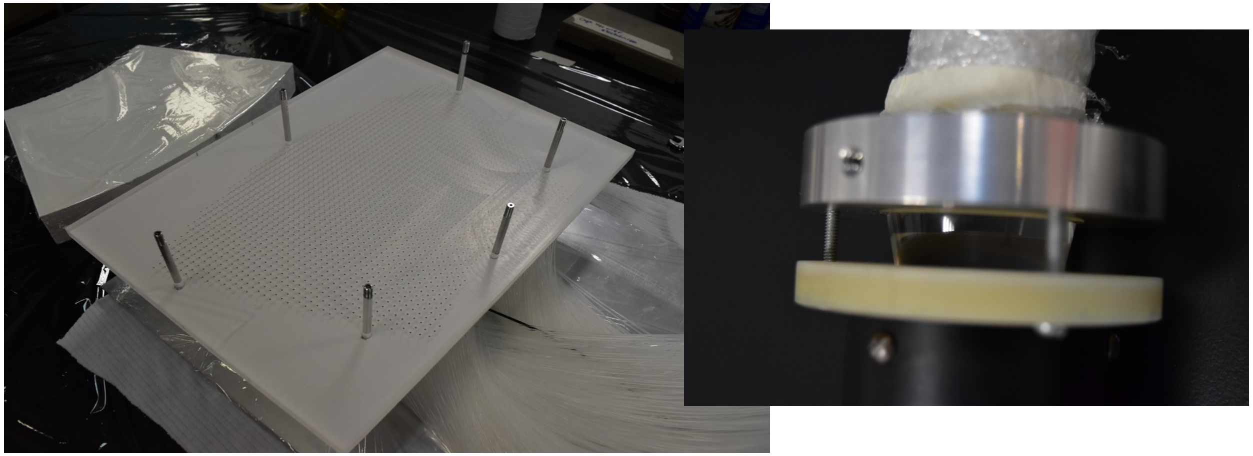

Test beam results for the forth Prototype

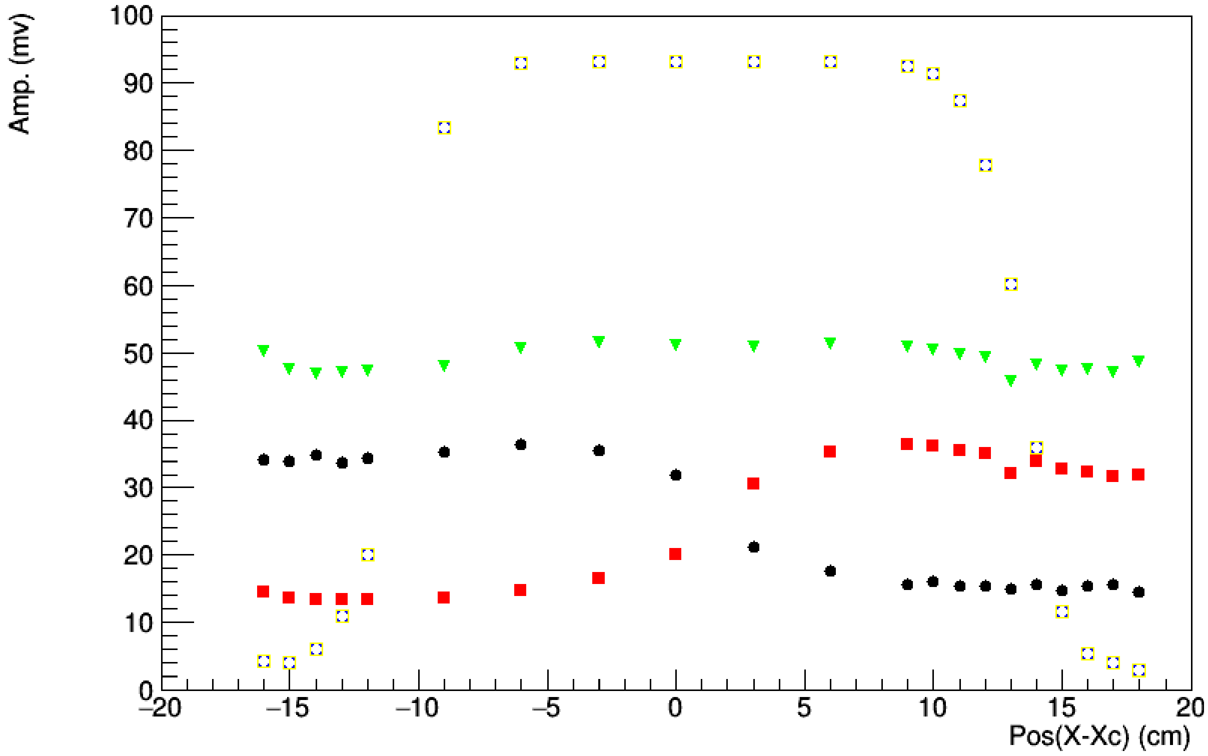

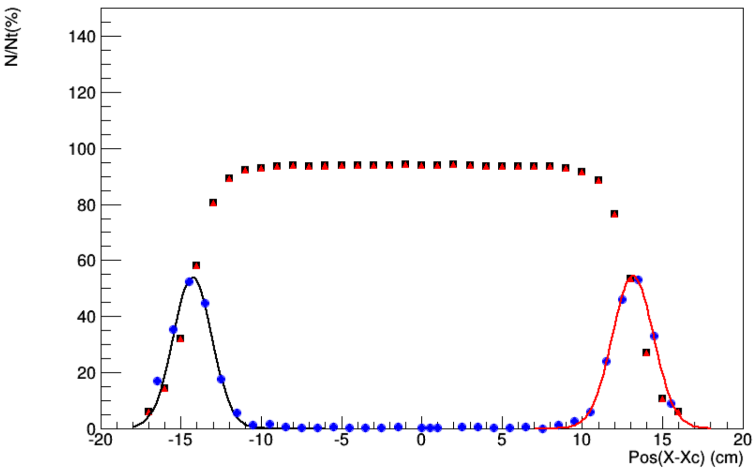

Sector Prototype

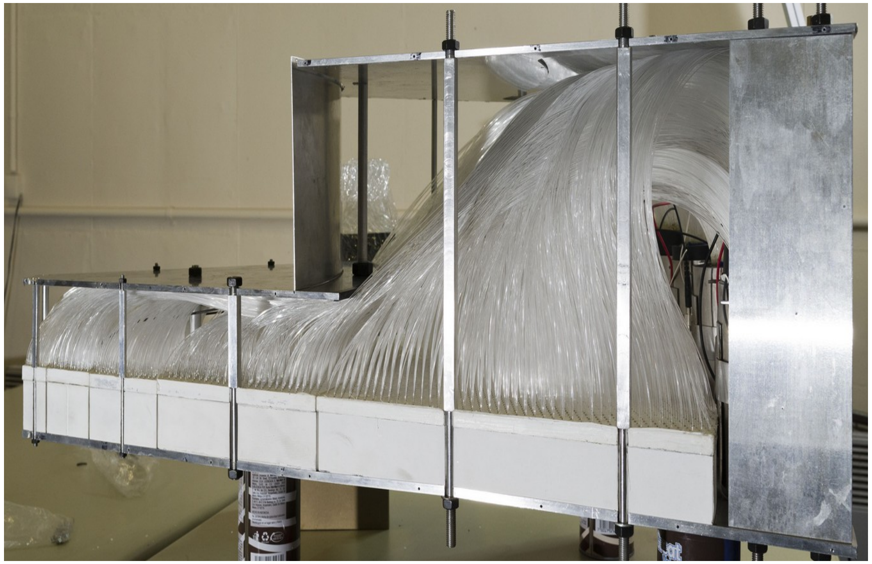

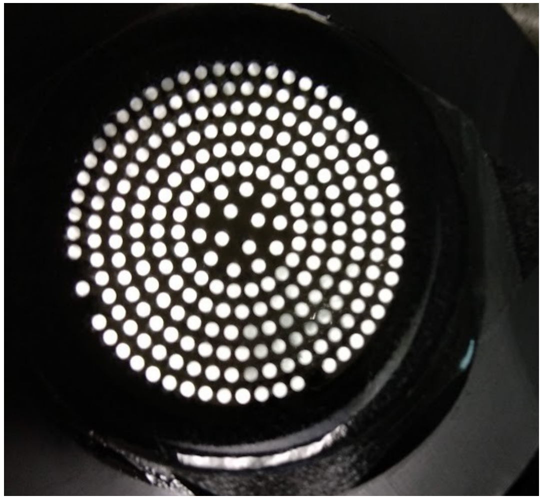

Sector Prototype

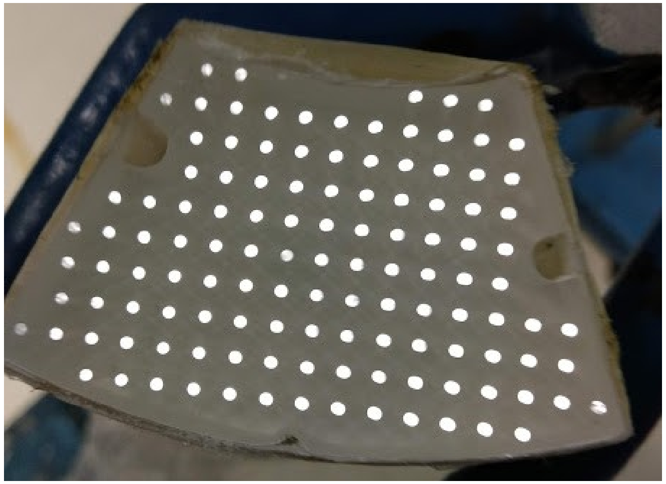

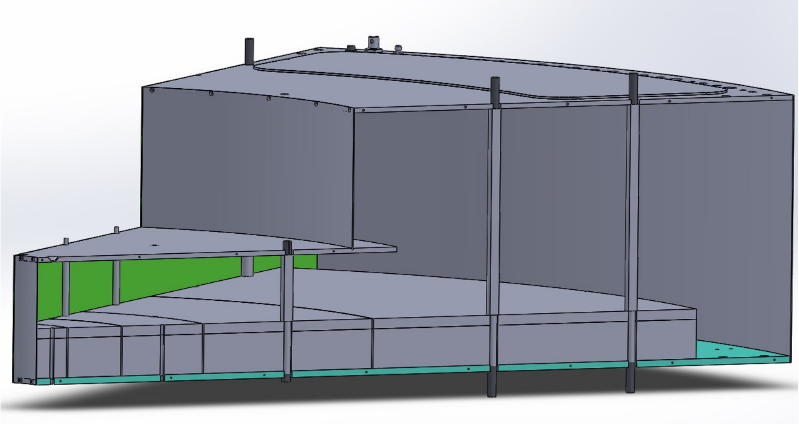

Test beam setup

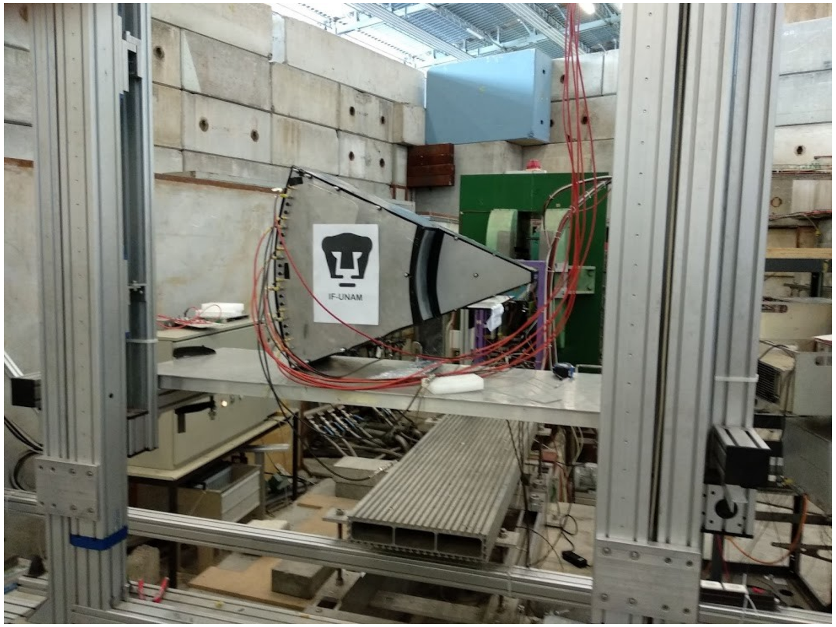

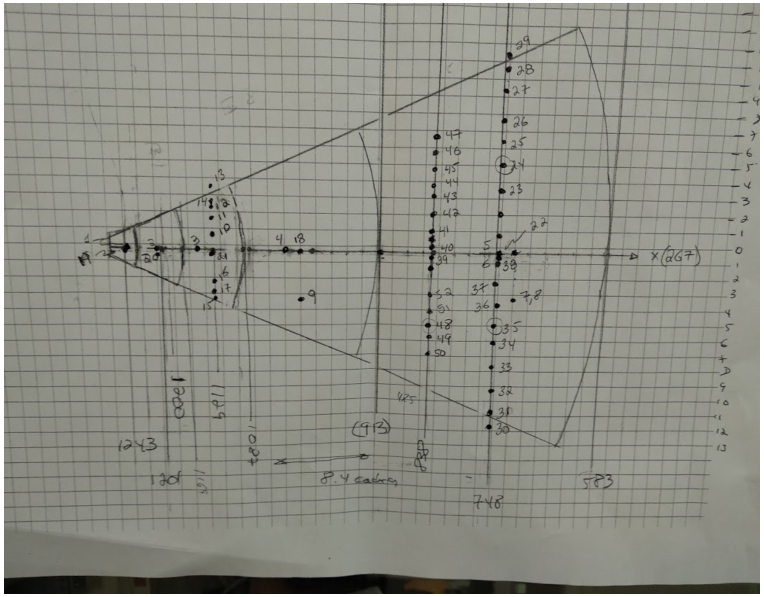

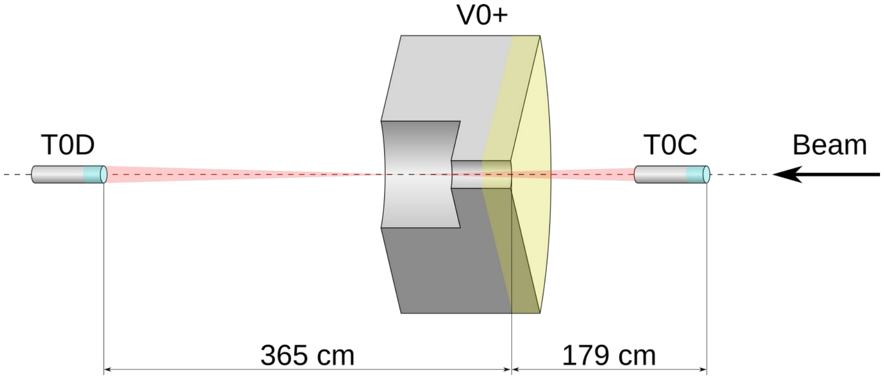

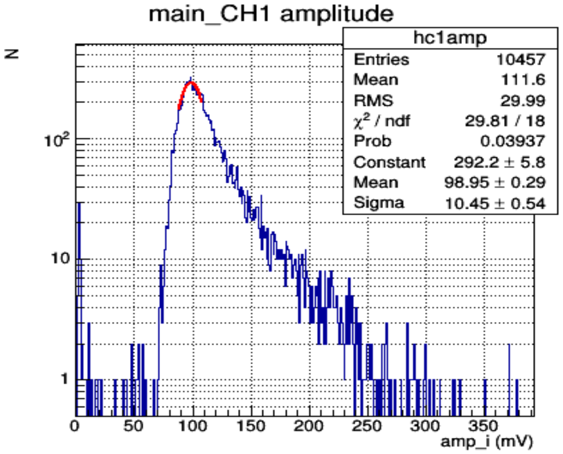

Test beam results for the Sector Prototype

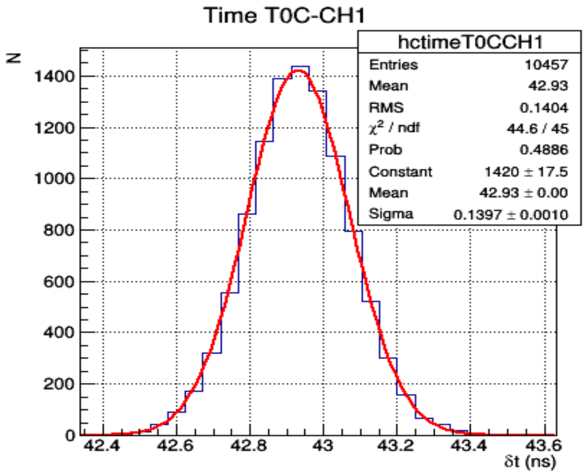

Fiber distance 3mm

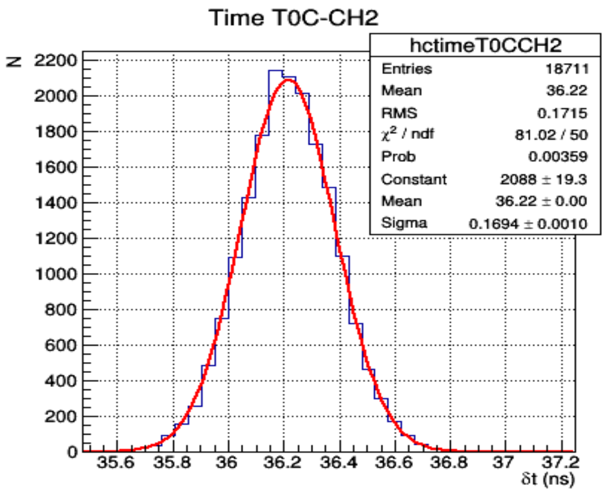

Fiber distance 4mm

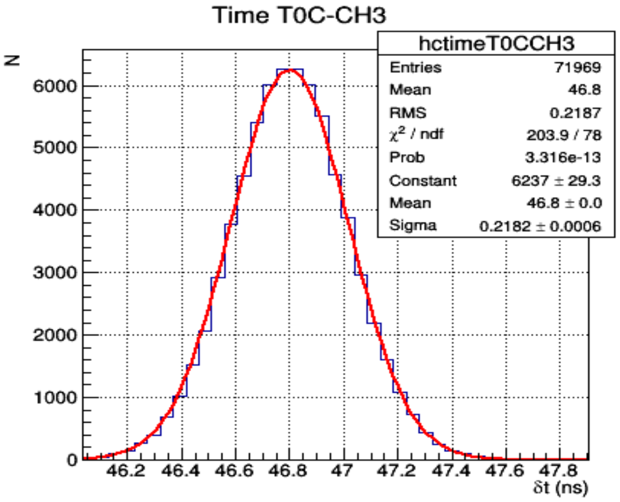

Fiber distance 5mm

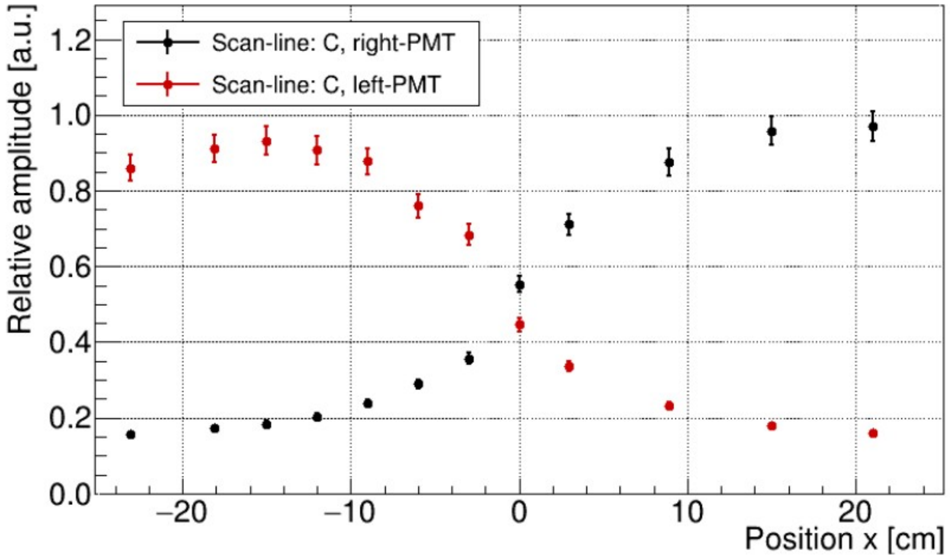

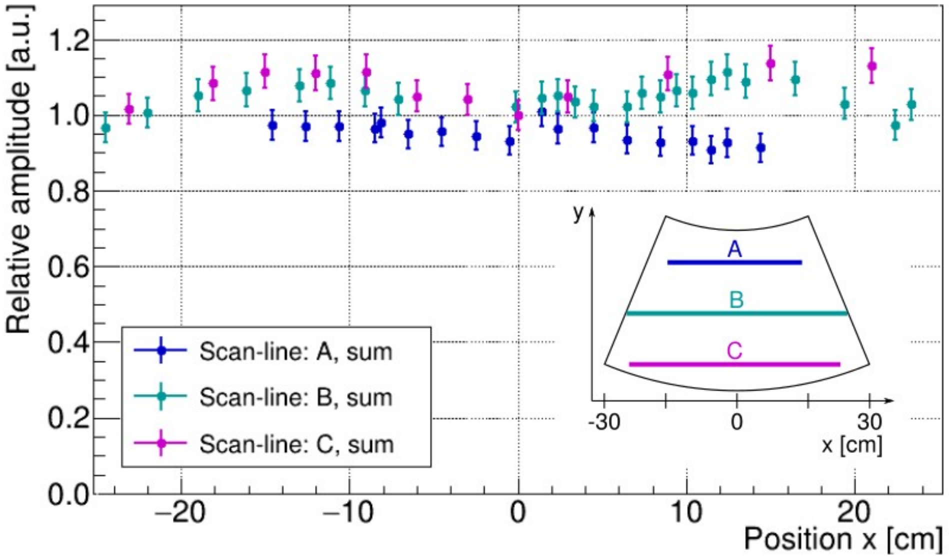

Normalized amplitudes in different positions

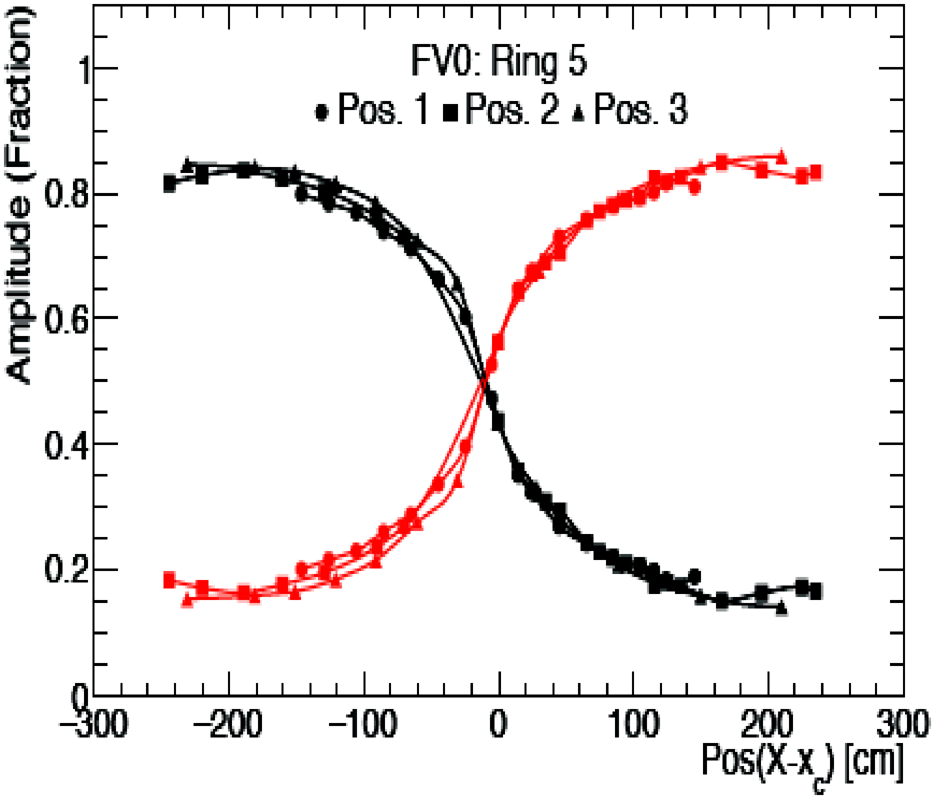

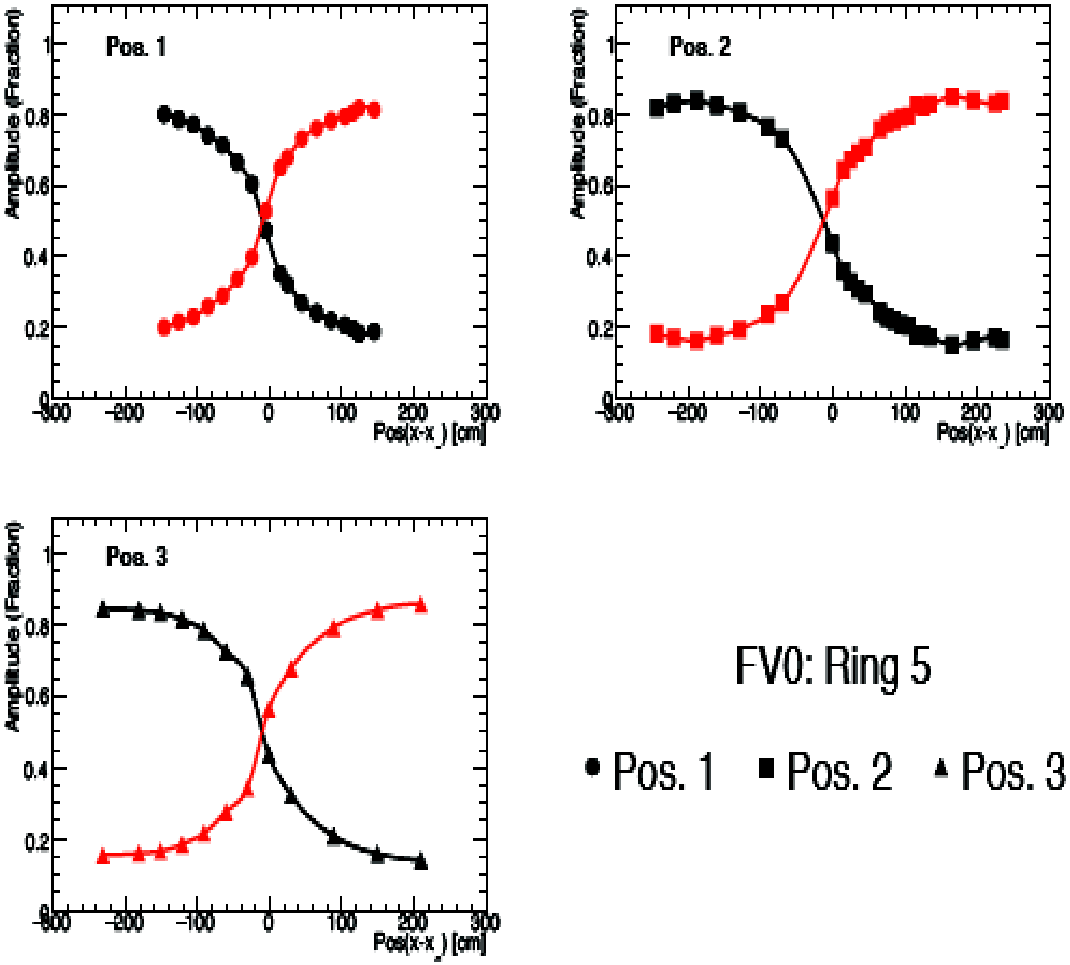

FV0: Ring 5

● Pos. 1 ■ Pos. 2 ▲ Pos. 3

Life time tests for 2” fine mesh

Similar to typical one below 1000 hours

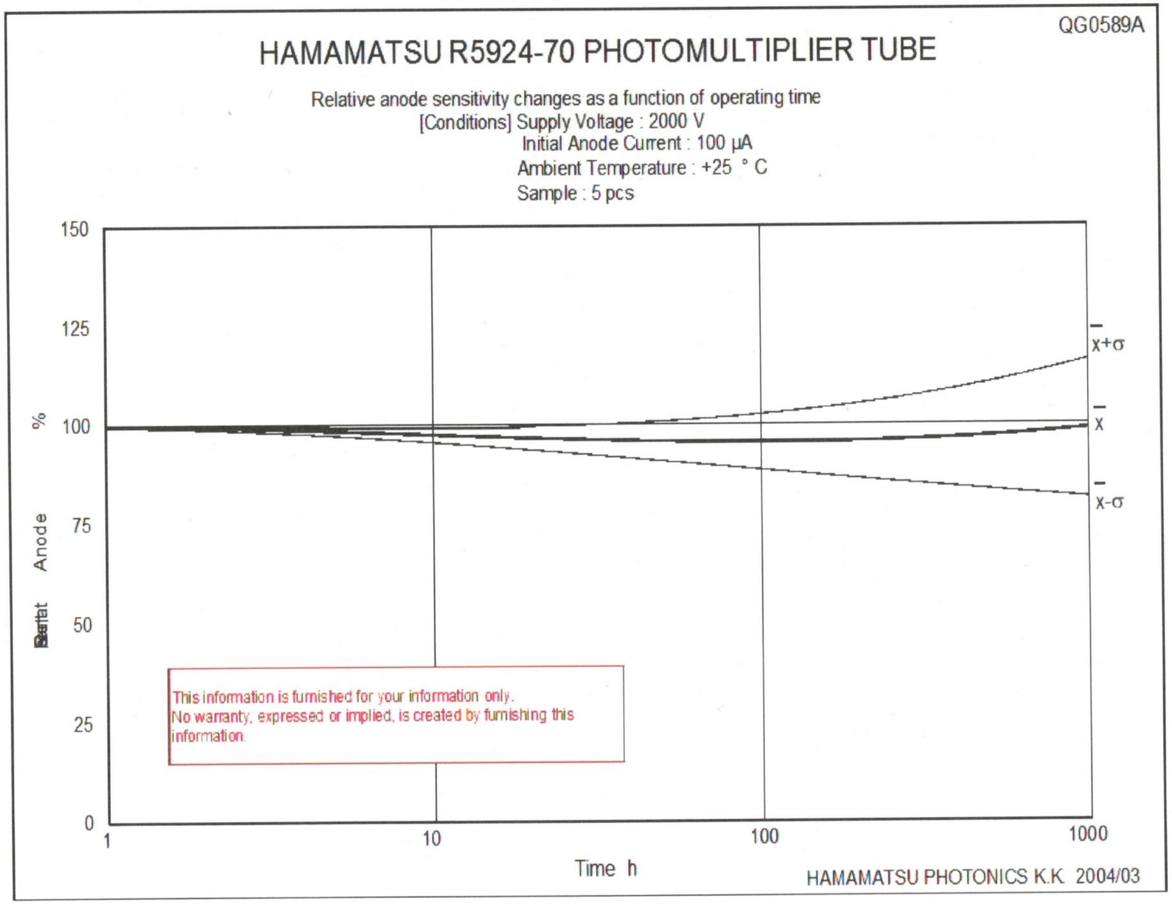

In average non stability is less than 5% after
1000hours or ~ 360C accumulated charge
Another +- 15% is the spread.
Comes from the sample of 5pcs

Test/Ref

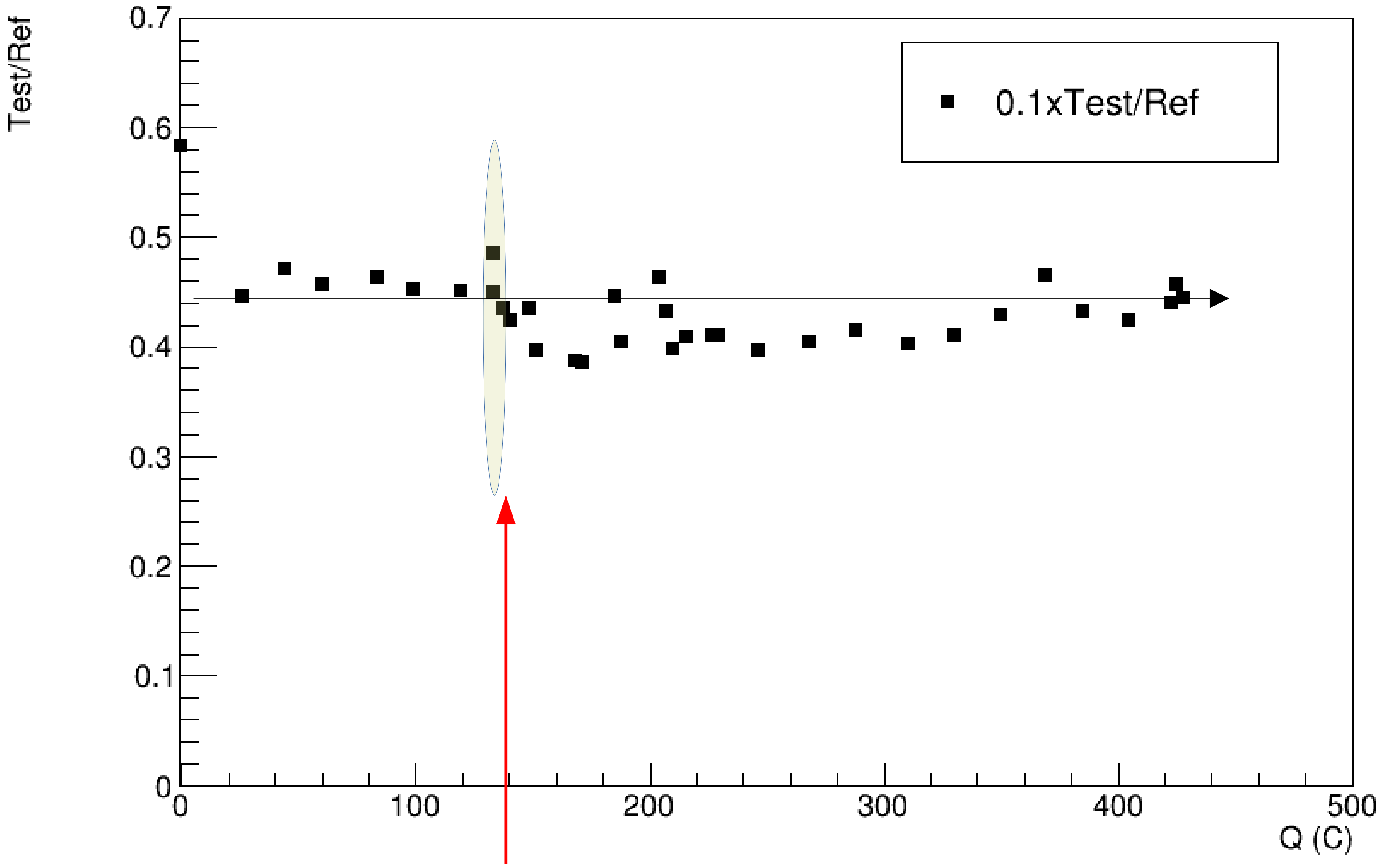

After 10 days stop

Anode current from rate scan

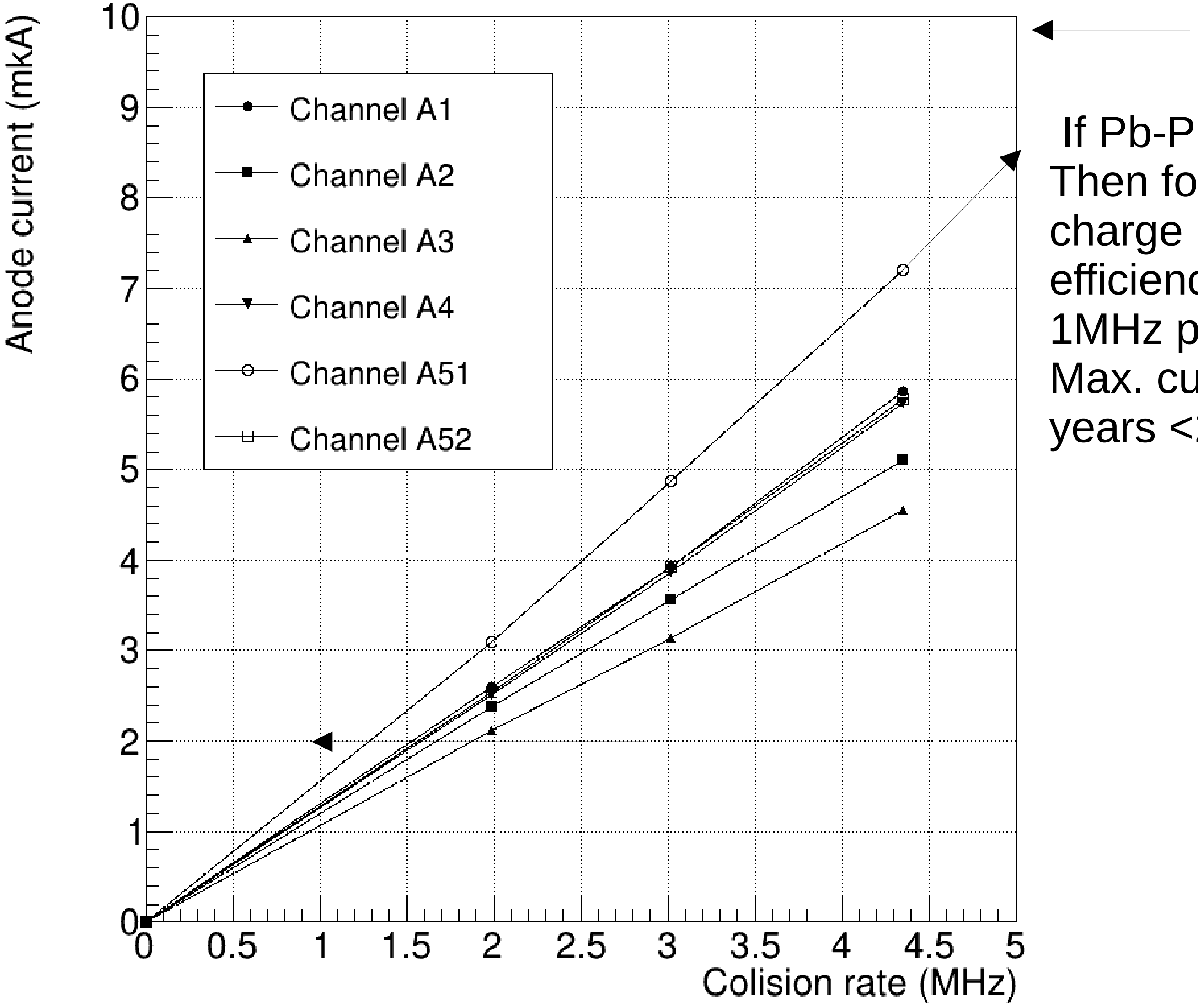

If Pb-Pb equivalent 5MHz pp
Then for 1monthh Pb-Pb Accumulated charge is less than 15C(50% efficiency). 10Years < 150C.
1MHz pp 10 months per year with 50% Max. curr. 2MkA. Accum. Q < 26C, 10 years <260C. Sum is less than 410C

Construction participants

Detector ensemble

After the installation

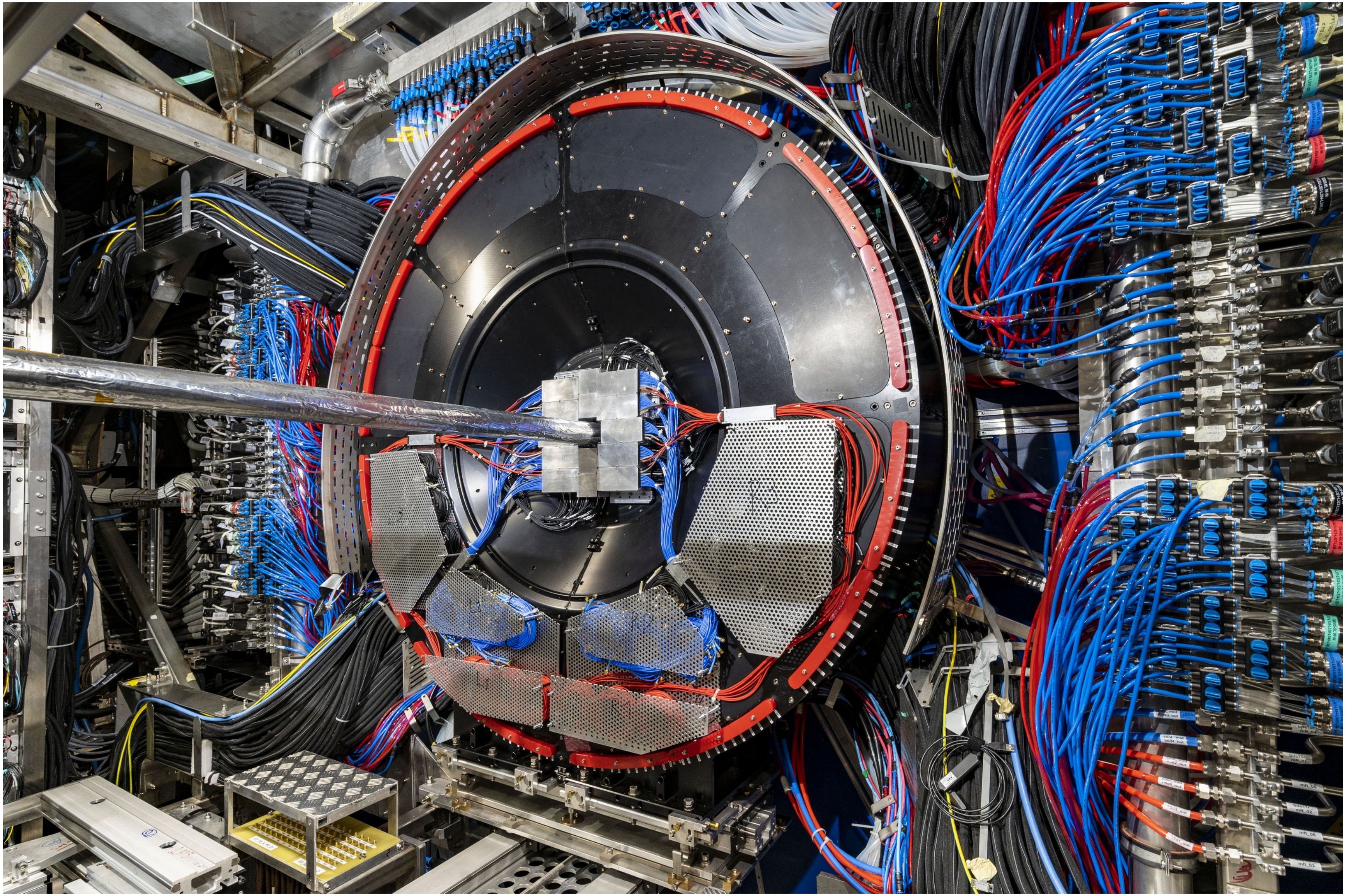

After the installation

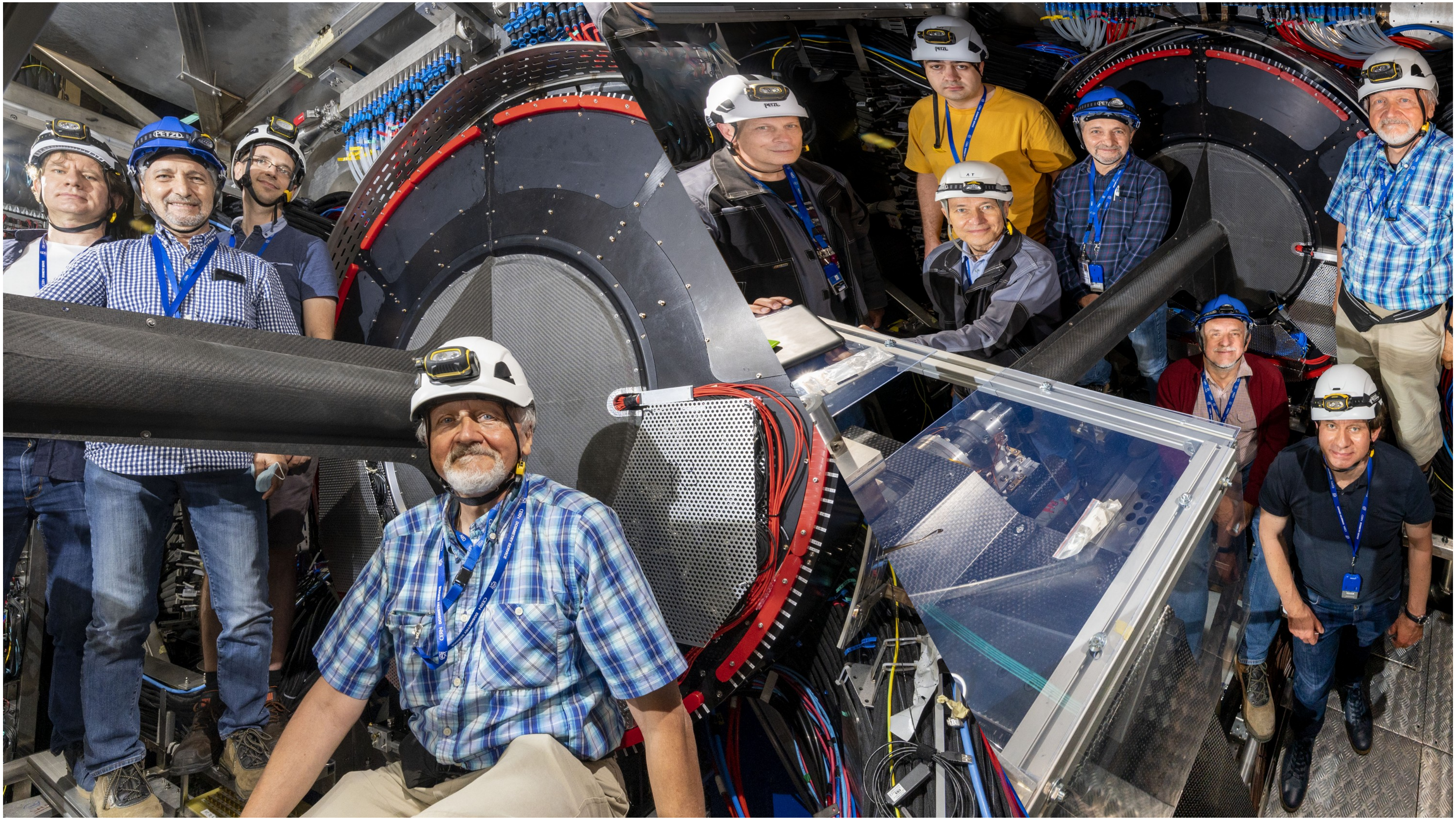

Some Beam Results

p-p

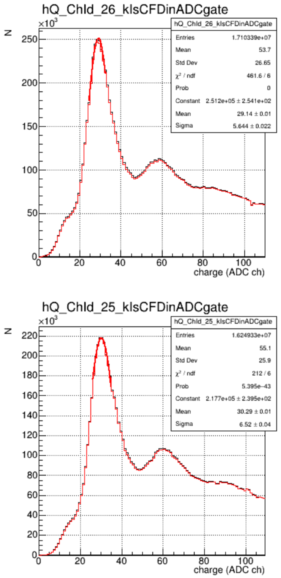

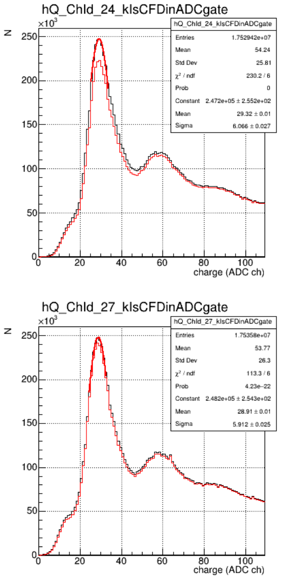

MIP = 32ch

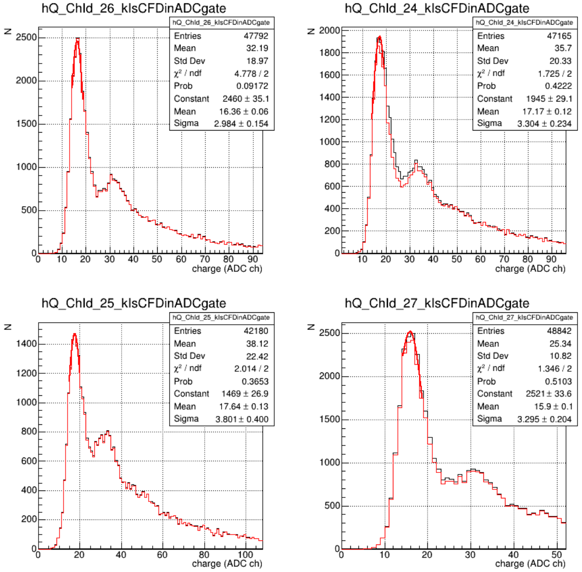

MIP = 17ch

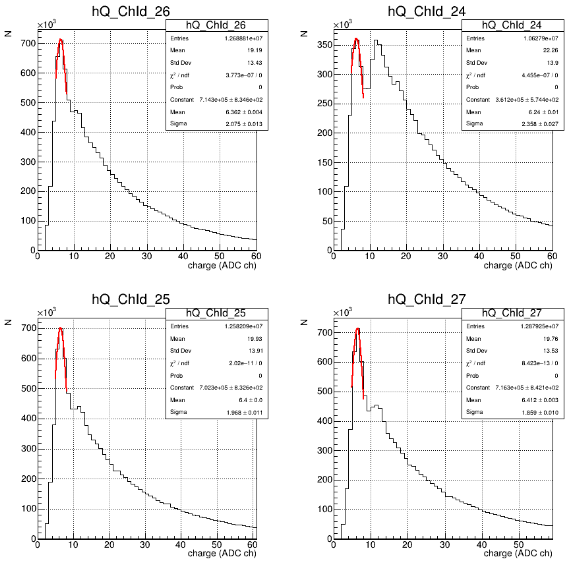

MIP = 6ch

Pb-Pb

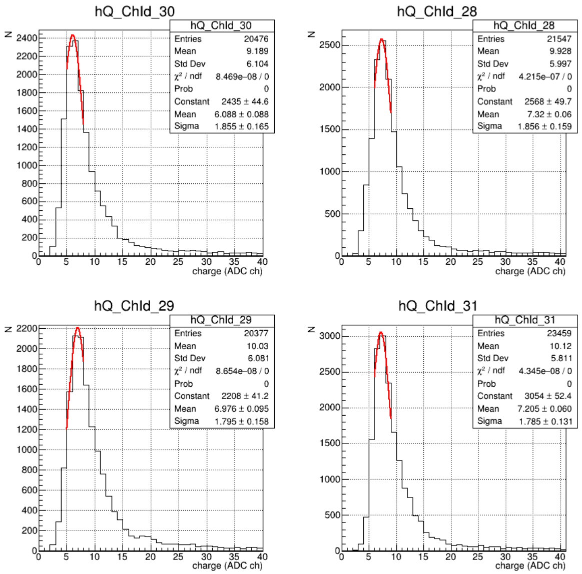

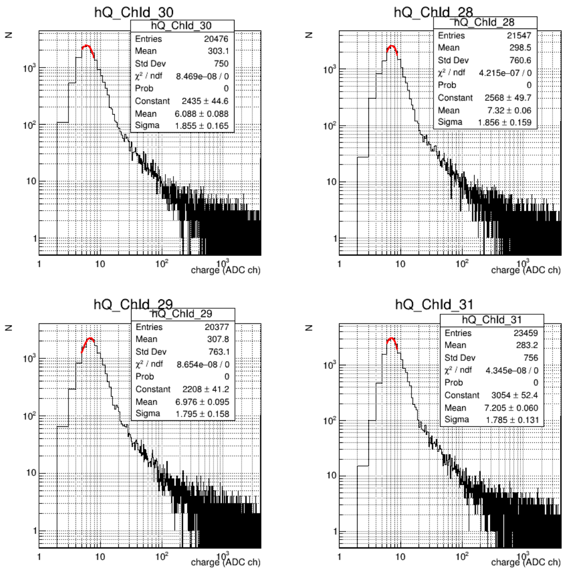

MIP = 6ch

V.Grabski

Some ideas on muonID

Keeping photo-sensor surface constant the collected light is independent from scintillator thickness

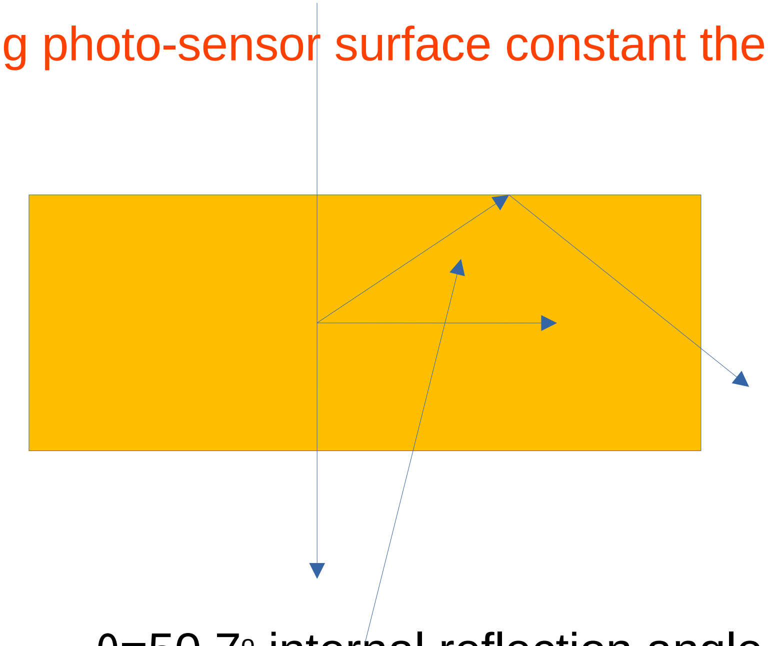

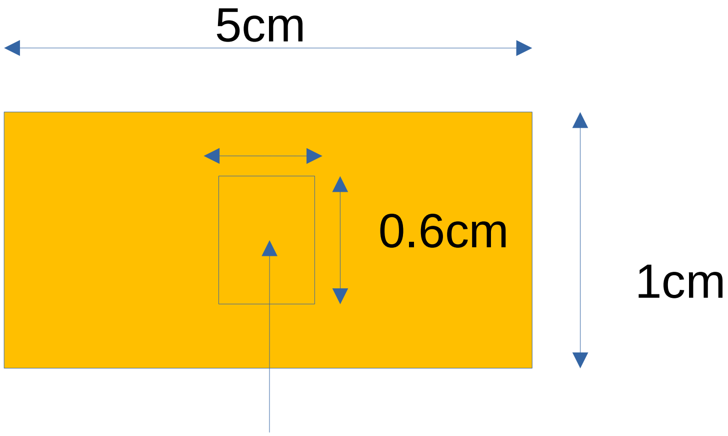

SiPM-6x6mm2

θ=50.7° internal reflection angle

Surface ratio=0.36/5=0.072

(1-cosθ)/2 ~0.18, in one side 18% of light is inside internal reflection.

Total min eff=0.18x0.072=0.013

1cm scint. ~10000ph

We should expect more light using reflective covers

130ph → 32-50PE

Some ideas on muonID

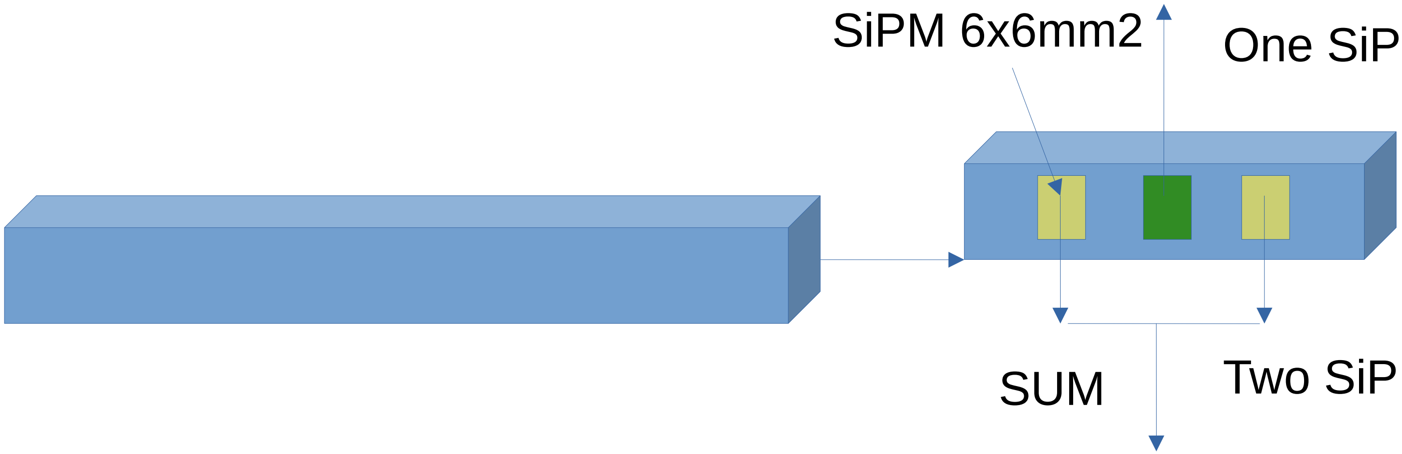

SiPM 6x6mm2

One SiPM

thickness to find

SUM

Two SiPM

Non uniform areas

Two SiPM or find a masking to make more uniform

Some ideas on muonID

Two scintillators with sizes 5x100x1cm & 5x100x1.7cm was cut and should be tested in the next year